

**SUPPORTING INFORMATION FOR**

**Highly phosphorescent Carbene-Metal-Carboranyl  
complexes of Copper(I) and Gold(I)**

Samuel L. Powley, Charlotte Riley, Hwan-Hee Cho, Nguyen Le Phuoc, Mikko Linnolahti,

Neil Greenham, and Alexander S. Romanov

## Supporting Information Table of Contents

### Table of Contents

General considerations	p. S3
Experimental and NMR spectroscopy	p. S4
TGA curves for the complexes	p. S18
X-ray Crystallography	p. S19
Electrochemistry	p. S23
Photophysical characterisation	p. S25
OLED device fabrication	p. S29
Computational details	p. S31

## GENERAL CONSIDERATIONS

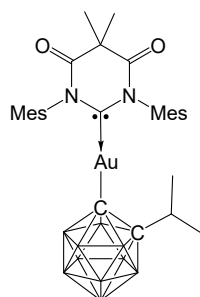
All reactions were performed under a N<sub>2</sub> atmosphere. Solvents were dried as required. 1-Ph-1,2-C<sub>2</sub>B<sub>10</sub>H<sub>11</sub>,<sup>1</sup> (MesDAC)AuCl,<sup>2</sup> (DippDAC)AuCl<sup>2</sup> and [(MesDACCuCl)<sub>2</sub>]<sup>3</sup> were prepared by literature methods or slight variations thereof. <sup>1</sup>H, <sup>11</sup>B{<sup>1</sup>H} and <sup>13</sup>C NMR spectra were recorded on a Bruker AVIII HD 400 MHz or AV II 700 MHz spectrometer. <sup>1</sup>H and <sup>13</sup>C NMR spectra were referenced to CD<sub>2</sub>Cl<sub>2</sub> at δ 5.32 (<sup>13</sup>C δ 53.84). Elemental analyses were performed by the Microanalysis Laboratory at the University of Manchester. Mass spectrometry data was obtained on a Thermo Orbitrap Exactive Plus Extended Mass Range Spectrometer using an APCI(ASAP) probe by the Mass Spectrometry Laboratory at the University of Manchester. All electrochemical experiments were performed using an Autolab PGSTAT 302N computer-controlled potentiostat. Cyclic voltammetry (CV) was performed using a three-electrode configuration consisting of a glassy carbon macrodisk working electrode (GCE) (diameter of 3 mm; BASi, Indiana, U.S.A.) combined with a Pt wire counter electrode (99.99%; GoodFellow, Cambridge, U.K.) and an Ag wire pseudoreference electrode (99.99%; GoodFellow, Cambridge, U.K.). The GCE was polished between experiments using alumina slurry (0.3 μm), rinsed in distilled water and subjected to brief sonication to remove any adhering alumina microparticles. The metal electrodes were then dried in an oven at 100 °C to remove residual traces of water, the GCE was left to air dry and residual traces of water were removed under vacuum. The Ag wire pseudoreference electrodes were calibrated to the ferrocene/ferrocenium couple in 1,2-difluorobenzene (DFB) at the end of each run to allow for any drift in potential, following IUPAC recommendations.<sup>4</sup> All electrochemical measurements were performed at ambient temperatures under an inert N<sub>2</sub> atmosphere in 1,2-difluorobenzene (DFB) containing the complex under study (0.14 mM) and the supporting electrolyte [*n*-Bu<sub>4</sub>N][PF<sub>6</sub>] (0.13 mM). Data were recorded with Autolab NOVA software (v. 1.11). Thermogravimetric analysis was performed with a TA Instruments SDT650 simultaneous thermal analyser under a stream of nitrogen.

## Experimental.

### Synthesis of 1-iPr-1,2-C<sub>2</sub>B<sub>9</sub>H<sub>11</sub>

1-iPr-1,2-C<sub>2</sub>B<sub>9</sub>H<sub>11</sub> was prepared based on the methodology of Valliant et al.<sup>1</sup> 6,9-bis(acetonitrile)decaborane (2.0 g, 9.89 mmol), AgNO<sub>3</sub> (140 mg, 0.82 mmol), 3-methyl-1-butyne (2 mL, 19.6 mmol) and toluene (10 mL) were sealed in a nitrogen-flushed bomb flask and heated to 130 °C for 60 hours. After cooling, the volatiles were removed under vacuum and the residue purified by flash chromatography (silica, hexane) to give 1-iPr-1,2-C<sub>2</sub>B<sub>9</sub>H<sub>11</sub> as an analytically pure colourless oil (0.97 g, 5.21 mmol, 52%).

### Synthesis of (MesDAC)Au(iPr-carboranyl) Au1



1-iPr-1,2-C<sub>2</sub>B<sub>10</sub>H<sub>11</sub> (75mg, 0.40 mmol) in 10 mL THF was cooled to 0°C, treated with nBuLi (0.18 mL of 2.5M solution, 0.44 mmol) and stirred at room temperature for 30 minutes. This solution was cooled to -78°C and (MesDAC)AuCl (245mg, 0.40 mmol) in 10 mL THF was slowly added. The reaction vessel was protected from light and stirred for 1 hour at -78°C and 1 hour at room temperature. The volatiles were removed *in vacuo*, the residue taken up in CH<sub>2</sub>Cl<sub>2</sub> and passed through a short plug of celite and silica. The eluent was reduced in volume to ca. 5 mL whereupon addition of hexane gave a white precipitate which was collected and washed with pentane. Trace impurities were removed by column chromatography (silica, 2:3 CH<sub>2</sub>Cl<sub>2</sub>/hexane) to give the product as a white solid (204 mg, 0.27 mmol, 67%). Diffraction-quality crystals were grown by slow diffusion of hexane into a concentrated CH<sub>2</sub>Cl<sub>2</sub> solution.

$^1\text{H}$  NMR ( $\text{CD}_2\text{Cl}_2$ , 400 MHz):  $\delta$  7.05 (s, 4H, Mes CH), 2.5-0.8 (br m, 10H, BH envelope), 2.35 (s, 6H, Mes p- $\text{CH}_3$ ), 2.13 (s, 12H, Mes o- $\text{CH}_3$ ), 1.78 (s, 6H, backbone  $\text{C}(\text{CH}_3)_2$ ), 1.34 (apparent quintet,  $J = 6.9$  Hz, 1H,  $^i\text{Pr}$  CH), 0.80 (d,  $J = 6.9$  Hz, 6H,  $^i\text{Pr}$   $\text{CH}_3$ ).

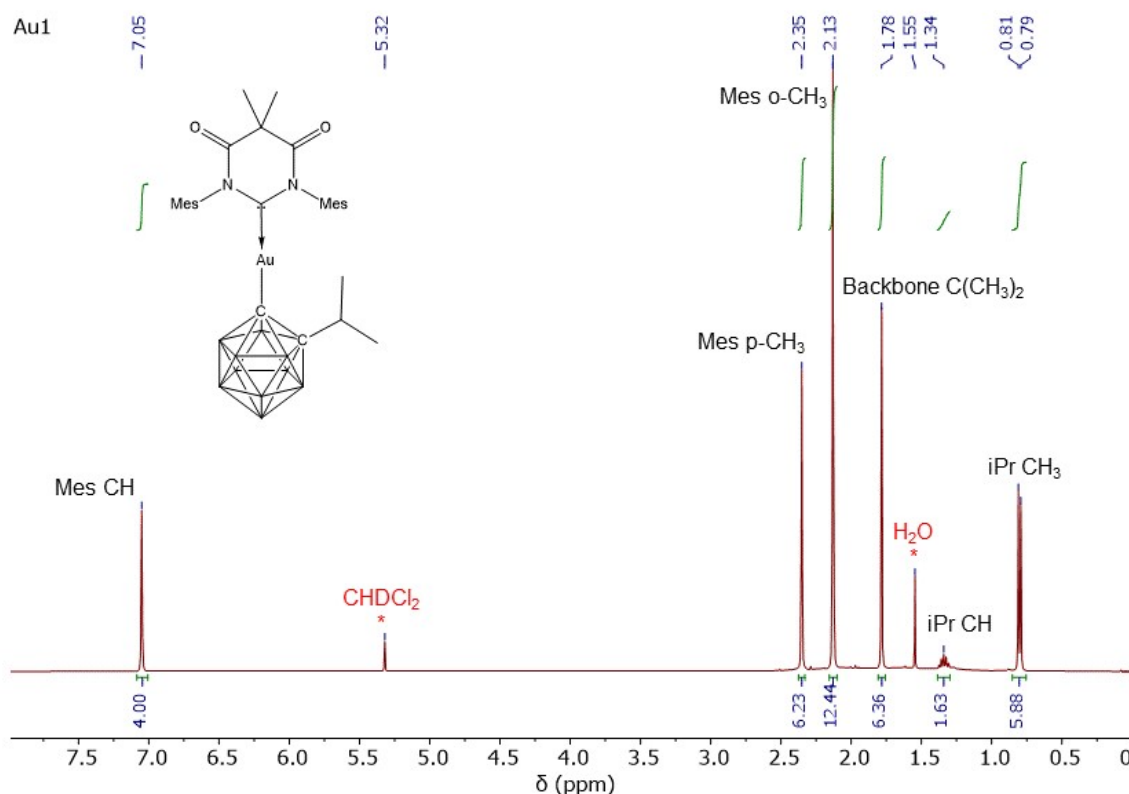
$^{11}\text{B}\{^1\text{H}\}$  NMR ( $\text{CD}_2\text{Cl}_2$ , 128.4 MHz):  $\delta$  -3.5, -5.6, -8.4, -10.1, -12.2.

$^{13}\text{C}\{^1\text{H}\}$  NMR ( $\text{CD}_2\text{Cl}_2$ , 100.6 MHz):  $\delta$  219.11 (carbene C), 171.61 ( $\text{C}=\text{O}$ ), 140.89 (Mes p-C), 135.05 (Mes o-C), 134.70 (Mes i-C), 130.18 (Mes m-CH), 95.88 (carborane  $\underline{\text{C}}\text{Au}$ ), 86.45 (carborane  $\underline{\text{C}}^i\text{Pr}$ ), 52.03 (backbone  $\underline{\text{C}}(\text{CH}_3)_2$ ), 37.97 (carborane  $^i\text{Pr}$  CH), 24.93 (backbone  $\text{C}(\underline{\text{C}}\text{H}_3)_2$ ), 24.53 (carborane  $^i\text{Pr}$   $\text{CH}_3$ ), 21.26 (Mes p- $\text{CH}_3$ ), 18.18 (Mes o- $\text{CH}_3$ ).

HRMS:  $\text{C}_{29}\text{H}_{45}\text{B}_{10}\text{N}_2\text{O}_2\text{Au}$  theoretical  $[\text{M}+\text{H}]^+$ : 759.4239; found (APCI(ASAP)): 759.4239.

Anal. Calcd. For  $\text{C}_{29}\text{H}_{46}\text{B}_{10}\text{N}_2\text{O}_2\text{Au}$ : C 45.85, H 6.10, N 3.69. Found: C 45.72, H 5.80, N 3.53.

#### Au1 $^1\text{H}$ NMR (400 MHz, $\text{CD}_2\text{Cl}_2$ )



**Au1**

**11B{**

**1H}**

**NM**

**R**

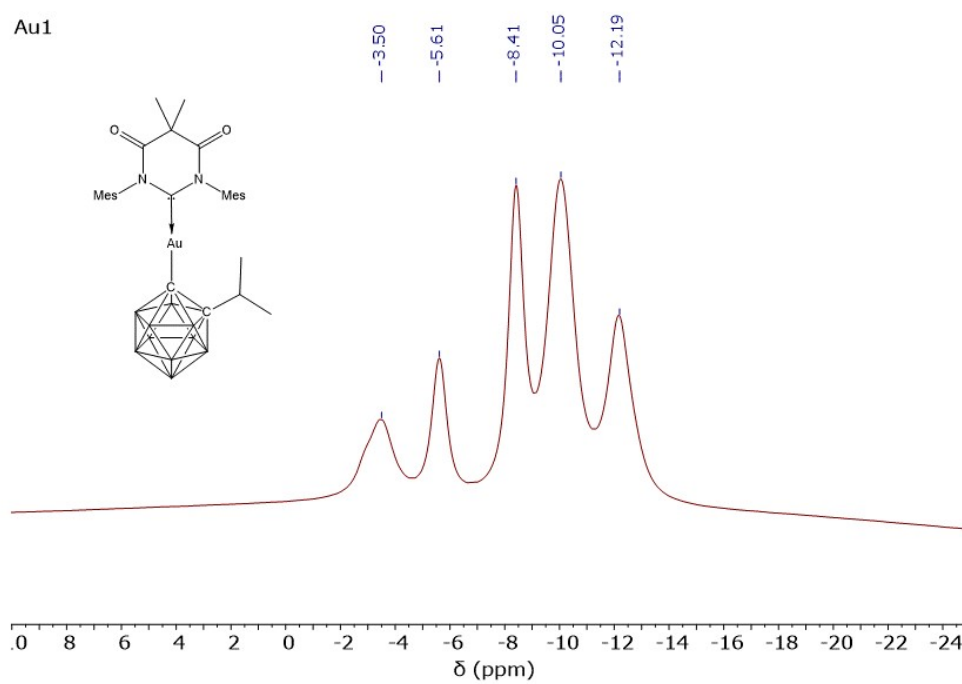
**(128.**

**4**

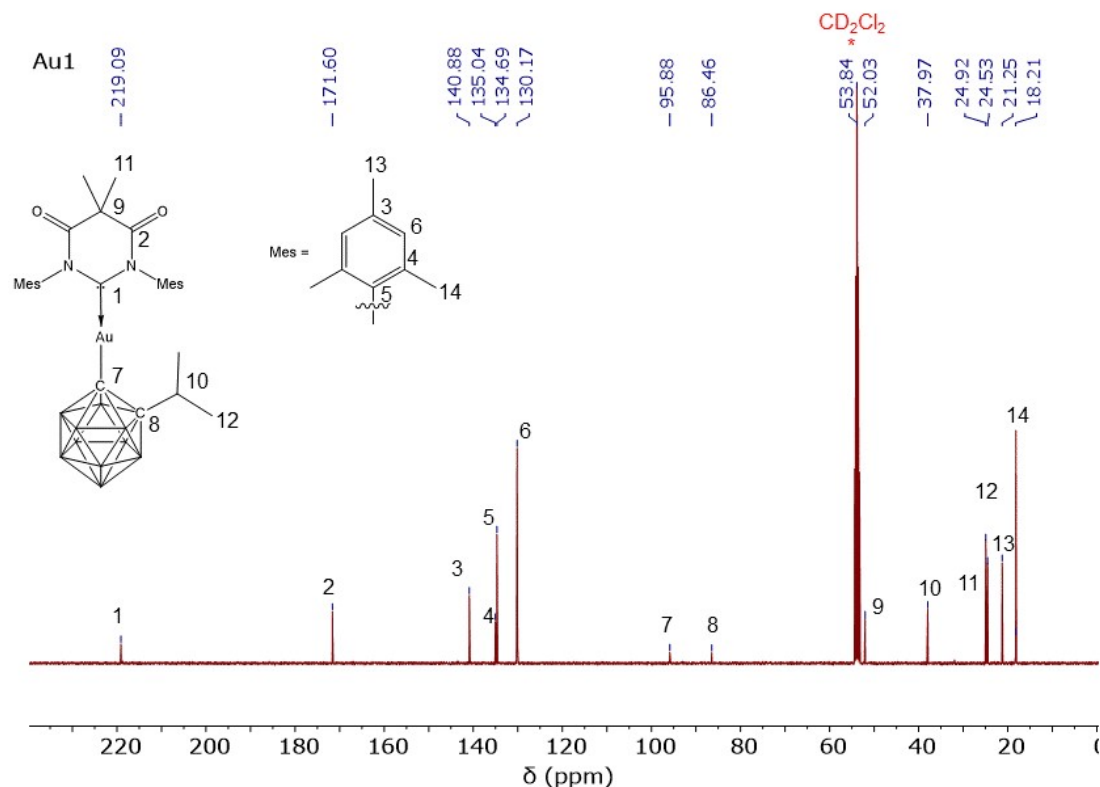
**MHz,**

**CD<sub>2</sub>**

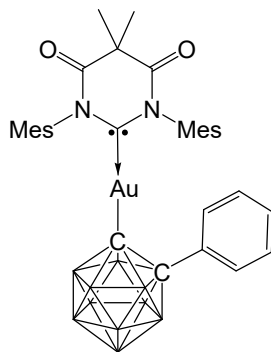
**Cl<sub>2</sub>)**



**Au1 <sup>13</sup>C{<sup>1</sup>H} NMR (100.6 MHz, CD<sub>2</sub>Cl<sub>2</sub>)**



### Synthesis of (MesDAC)Au(Ph-carboranyl) Au2



A solution of 1-Ph-1,2-C<sub>2</sub>B<sub>10</sub>H<sub>11</sub> (50 mg, 0.23 mmol) in THF (5 mL) was cooled to 0°C and treated with 2.5M nBuLi solution (0.10 mL, 0.25 mmol). After stirring for 30 minutes, the solution was cooled to -78°C and a solution of (MesDAC)AuCl (118 mg, 0.19 mmol) in THF (10 mL) was added slowly. The mixture was stirred for 10 minutes at -78°C then warmed to RT and evaporated to dryness under vacuum. The residue was passed through a short plug of celite and silica using CH<sub>2</sub>Cl<sub>2</sub> eluent, concentrated, and purified by column chromatography

(silica, 2:3 CH<sub>2</sub>Cl<sub>2</sub>/hexane) to give (MesDAC)Au(Ph-carboranyl) as a white solid (76 mg, 0.10 mmol, 51%). Diffraction-quality crystals were grown by slow diffusion of hexane into a concentrated CH<sub>2</sub>Cl<sub>2</sub> solution.

<sup>1</sup>H NMR (CD<sub>2</sub>Cl<sub>2</sub>, 400 MHz): δ 7.34 (m, 3H, Ph CH), 7.20 (app t, *J* = 7.7 Hz, 2H, Ph CH), 2.9-0.9 (br m, 10H, BH envelope), 2.41 (s, 6H, Mes p-CH<sub>3</sub>), 1.90 (s, 12H, Mes o-CH<sub>3</sub>), 1.71 (s, 6H, backbone C(CH<sub>3</sub>)<sub>2</sub>).

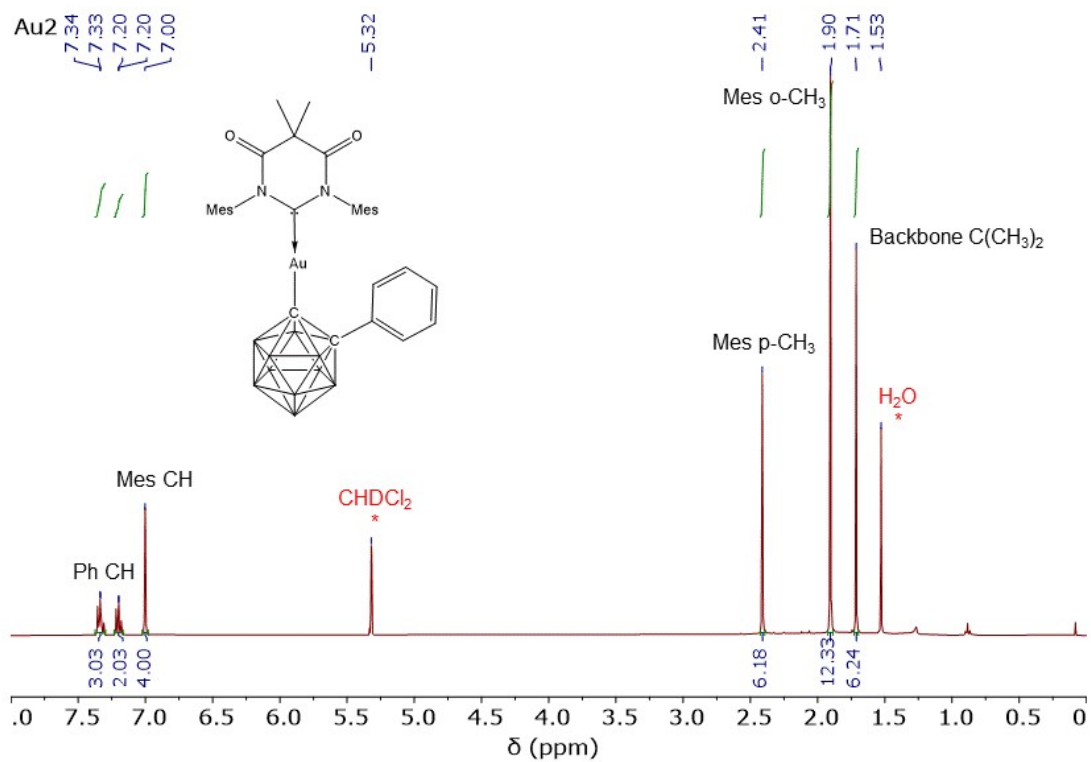
<sup>11</sup>B{<sup>1</sup>H} NMR (CD<sub>2</sub>Cl<sub>2</sub>, 128.4 MHz): δ -2.1, -4.8, -8.3, -9.5.

<sup>13</sup>C{<sup>1</sup>H} NMR (CD<sub>2</sub>Cl<sub>2</sub>, 100.6 MHz): δ 219.26 (carbene C), 171.52 (C=O), 140.80 (Mes p-C), 138.08 (Ph i-C), 135.07 (Mes o-C), 134.57 (Mes i-C), 130.10 (Mes m-CH), 130.00 (Ph m/p-CH), 129.07 (Ph m/p-CH), 128.15 (Ph o-CH), 96.62 (carborane C<sub>Au</sub>), 82.40 (carborane C<sup>i</sup>Pr), 51.95 (backbone C(CH<sub>3</sub>)<sub>2</sub>), 24.92 (backbone C(CH<sub>3</sub>)<sub>2</sub>), 21.27 (Mes p-CH<sub>3</sub>), 18.10 (Mes o-CH<sub>3</sub>).

HRMS: C<sub>32</sub>H<sub>43</sub>B<sub>10</sub>N<sub>2</sub>O<sub>2</sub>Au theoretical [M+H]<sup>+</sup>: 793.4081; found (APCI(ASAP)): 793.4063.

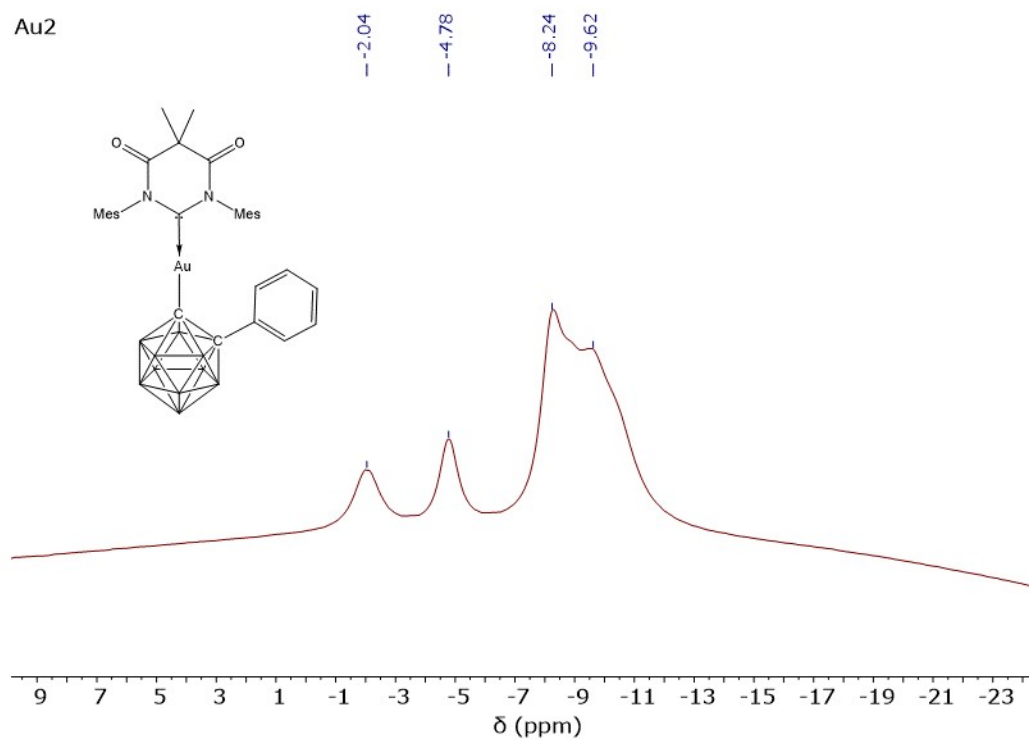
Anal. Calcd. For C<sub>32</sub>H<sub>43</sub>B<sub>10</sub>N<sub>2</sub>O<sub>2</sub>Au: C 48.48, H 5.47, N 3.53. Found: C 48.34, H 5.53, N 3.79.



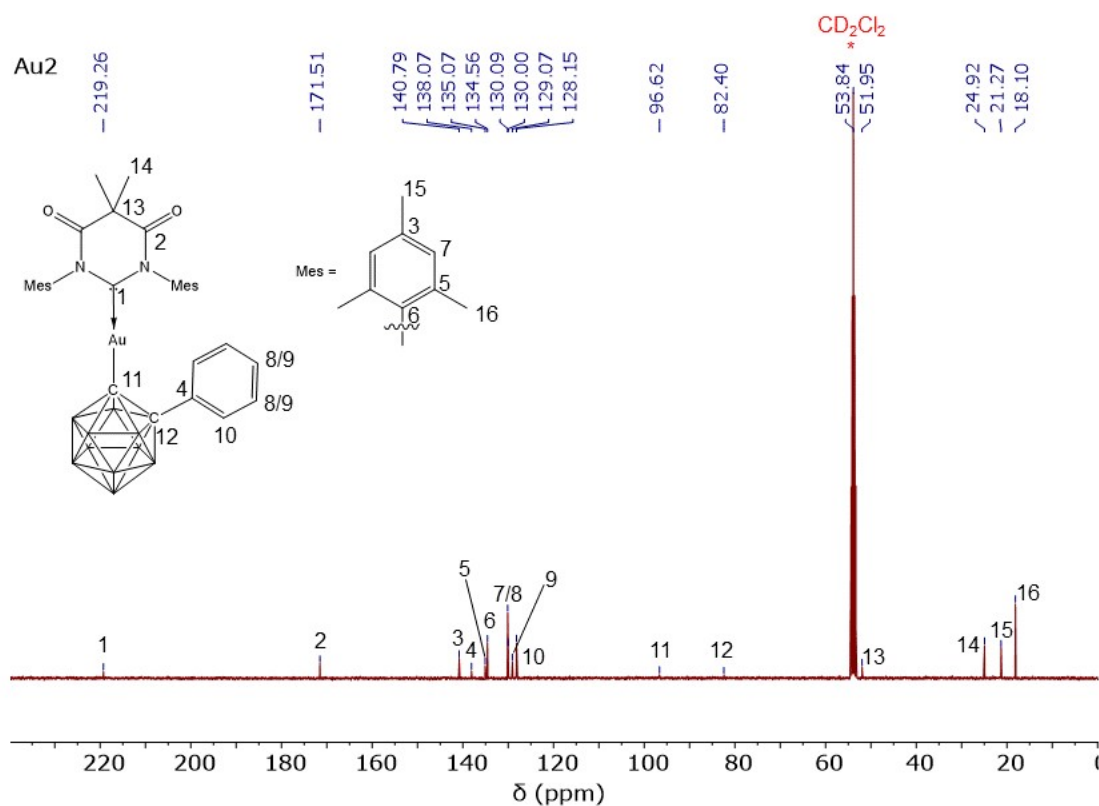


**Au2 <sup>1</sup>H NMR (400 MHz, CD<sub>2</sub>Cl<sub>2</sub>)**

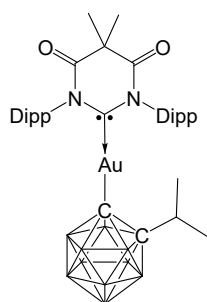
**Au2 <sup>11</sup>B{<sup>1</sup>H} NMR (128.4 MHz, CD<sub>2</sub>Cl<sub>2</sub>)**



### Au2 <sup>13</sup>C{<sup>1</sup>H} NMR (100.6 MHz, CD<sub>2</sub>Cl<sub>2</sub>)



### Synthesis of (DippDAC)Au(iPr-carboranyl) Au<sub>3</sub>



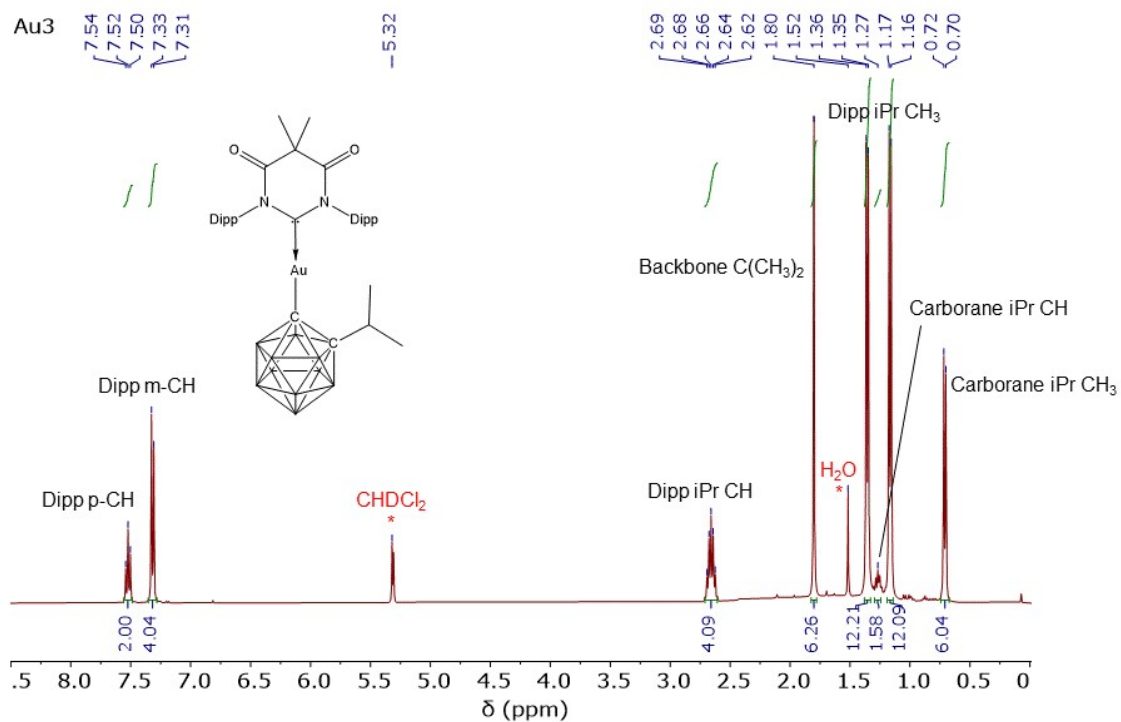
A solution of 1-Li-2-iPr-1,2-C<sub>2</sub>B<sub>10</sub>H<sub>10</sub> (0.26 mmol) in 5 mL THF, prepared from 1-iPr-1,2-C<sub>2</sub>B<sub>10</sub>H<sub>11</sub> (48 mg, 0.26 mmol) and 2.5M nBuLi (0.12 mL, 0.30 mmol), was cooled to -78°C and a solution of (DippDAC)AuCl (149 mg, 0.22 mmol) in THF (10 mL) was slowly added. The mixture was stirred at -78°C for 30 minutes and RT for 1 hour. All volatiles were removed *in vacuo* and the residue was taken up in CH<sub>2</sub>Cl<sub>2</sub> and filtered through a short layer of celite and

silica. The eluent was evaporated and the residue purified by column chromatography (silica, 2:3 CH<sub>2</sub>Cl<sub>2</sub>/hexane) to give (DippDAC)Au(iPr-carboranyl) as a white solid (84 mg, 0.10 mmol, 45%). Diffraction-quality crystals were grown by slow diffusion of hexane into a concentrated CH<sub>2</sub>Cl<sub>2</sub> solution.

<sup>1</sup>H NMR (CD<sub>2</sub>Cl<sub>2</sub>, 400 MHz): δ 7.52 (t, *J* = 7.8 Hz, 2H, Dipp p-CH), 7.32 (d, *J* = 7.7 Hz, 4H, Dipp m-CH), 2.7-0.9 (br m, 10H, BH envelope), 2.66 (sept, *J* = 6.9 Hz, 4H, Dipp <sup>i</sup>Pr CH), 1.80 (s, 6H, backbone C(CH<sub>3</sub>)<sub>2</sub>), 1.36 (d, *J* = 6.8 Hz, 12H, Dipp <sup>i</sup>Pr CH<sub>3</sub>), 1.27 (m, 1H, carborane <sup>i</sup>Pr CH), 1.17 (d, *J* = 6.8 Hz, 12H, Dipp <sup>i</sup>Pr CH<sub>3</sub>), 0.71 (d, *J* = 6.9 Hz, 6H, carborane <sup>i</sup>Pr CH<sub>3</sub>).

<sup>11</sup>B{<sup>1</sup>H} NMR (CD<sub>2</sub>Cl<sub>2</sub>, 128.4 MHz): δ -4.2, -5.7, -7.6, -10.0, -10.8, -12.2.

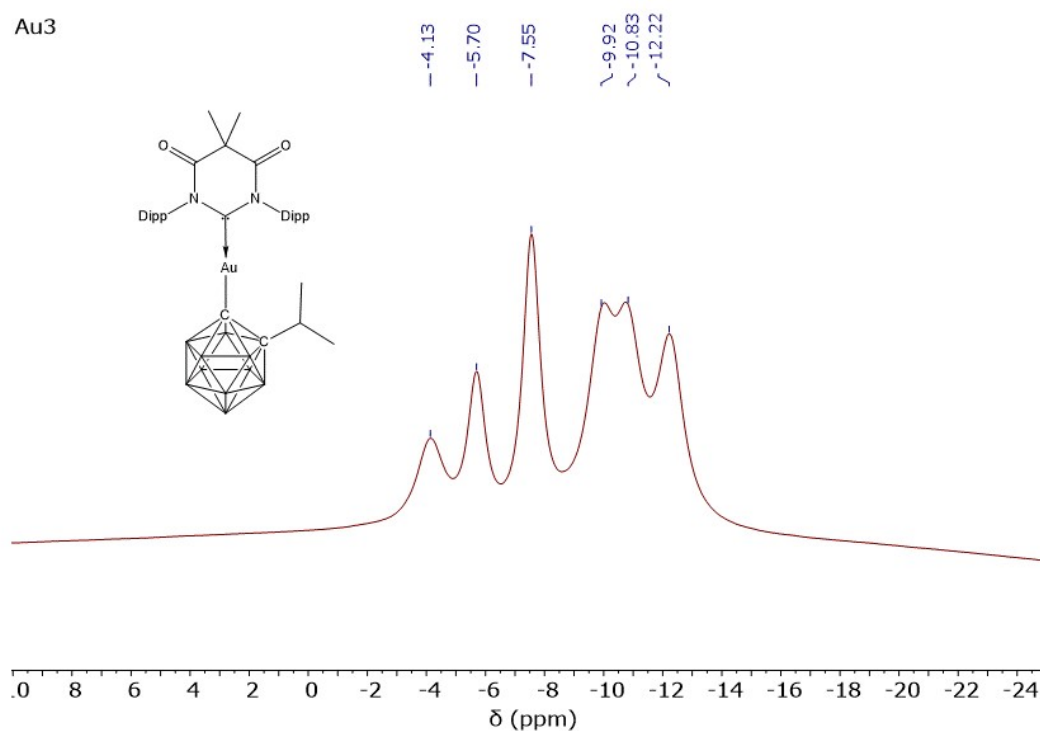
<sup>13</sup>C{<sup>1</sup>H} NMR (CD<sub>2</sub>Cl<sub>2</sub>, 100.6 MHz): δ 218.86 (carbene C), 172.43 (C=O), 145.35 (Dipp o-C), 134.53 (Dipp i-C), 131.41 (Dipp p-CH), 125.26 (Dipp m-CH), 99.96 (carborane CAu), 87.03 (carborane CPh), 51.73 (backbone C(CH<sub>3</sub>)<sub>2</sub>), 37.96 (carborane <sup>i</sup>Pr CH), 29.77 (Dipp <sup>i</sup>Pr CH), 25.30 (backbone C(CH<sub>3</sub>)<sub>2</sub>), 24.64 (carborane <sup>i</sup>Pr CH<sub>3</sub>), 24.40 (Dipp <sup>i</sup>Pr CH<sub>3</sub>), 23.68 (Dipp <sup>i</sup>Pr CH<sub>3</sub>). HRMS: C<sub>35</sub>H<sub>57</sub>B<sub>10</sub>N<sub>2</sub>O<sub>2</sub>Cu theoretical [M+H]<sup>+</sup>: 845.5135; found (APCI(ASAP)): 845.5137.

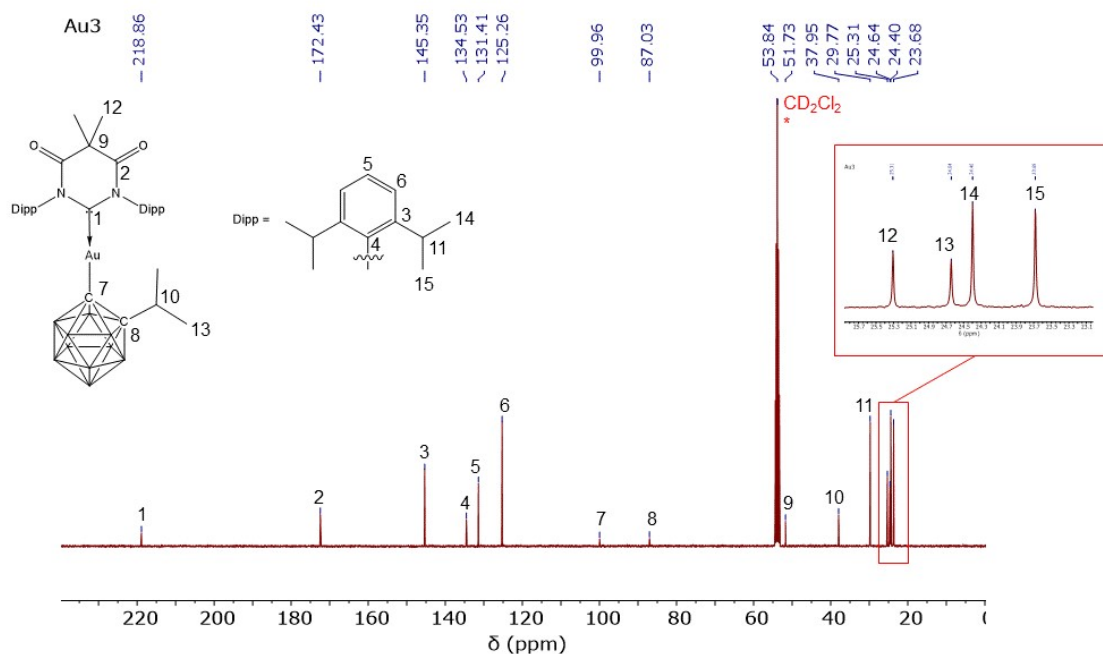


**Au3** <sup>1</sup>H NMR (400 MHz, CD<sub>2</sub>Cl<sub>2</sub>)

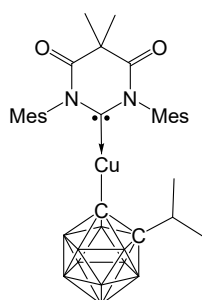
**Au3** <sup>11</sup>B{<sup>1</sup>H} NMR (128.4 MHz, CD<sub>2</sub>Cl<sub>2</sub>)

**Au3** <sup>13</sup>C{<sup>1</sup>H} NMR (100.6 MHz, CD<sub>2</sub>Cl<sub>2</sub>)





### Synthesis of (MesDAC)Cu(iPr-carboranyl) Cu1



A solution of 1-Li-2-iPr-1,2-C<sub>2</sub>B<sub>10</sub>H<sub>10</sub> (0.33 mmol) in 10 mL THF, prepared from 1-iPr-1,2-C<sub>2</sub>B<sub>10</sub>H<sub>11</sub> (62 mg, 0.33 mmol) and 2.5M nBuLi (0.15 mL, 0.38 mmol), was cooled to -78°C and a solution of [(MesDAC)CuCl]<sub>2</sub> (147 mg, 0.15 mmol) in THF (5 mL) was slowly added. The resulting red solution was allowed to slowly warm to RT and stir overnight. All volatiles were removed *in vacuo* and the residue was taken up in CH<sub>2</sub>Cl<sub>2</sub> and filtered through a short layer of celite and silica. The yellow eluent was concentrated and purified by column chromatography (silica, 1:4 ethyl acetate/hexane) to give (MesDAC)Cu(iPr-carboranyl) as a

yellow powder (79 mg, 0.13 mmol, 40.8%). Diffraction-quality crystals were grown from evaporation of a concentrated ethyl acetate/hexane solution.

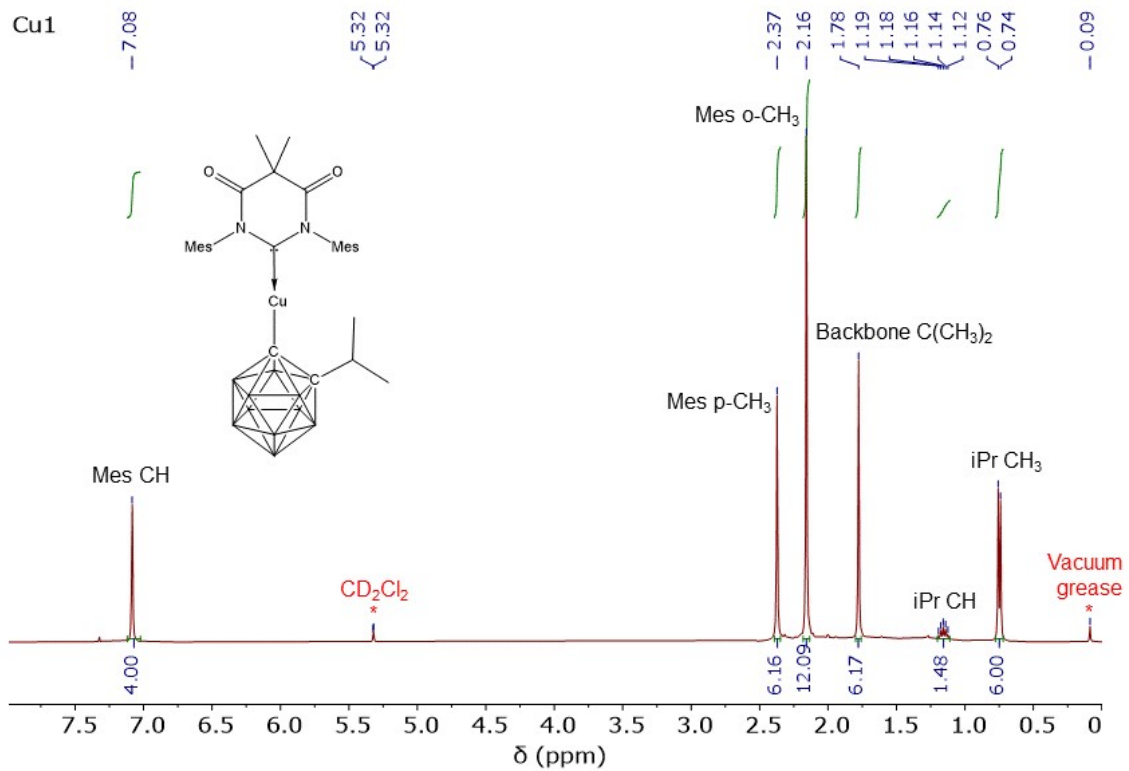
$^1\text{H}$  NMR ( $\text{CD}_2\text{Cl}_2$ , 400 MHz):  $\delta$  7.08 (s, 4H, Mes CH), 2.5-0.9 (br m, 10H, BH envelope), 2.37 (s, 6H, Mes p- $\text{CH}_3$ ), 2.16 (s, 12H, Mes o- $\text{CH}_3$ ), 1.78 (s, 6H, backbone  $\text{C}(\text{CH}_3)_2$ ), 1.16 (app. quintet,  $J = 6.9$  Hz, 1H,  $^i\text{Pr}$  CH), 0.75 (d,  $J = 6.9$  Hz, 6H,  $^i\text{Pr}$   $\text{CH}_3$ ).

$^{11}\text{B}\{1\text{H}\}$  NMR ( $\text{CD}_2\text{Cl}_2$ , 128.4 MHz):  $\delta$  -2.6 (1B), -5.6 (1B), -7.9 (2B), -10.8 (4B), -11.7 (2B).

$^{13}\text{C}\{1\text{H}\}$  NMR ( $\text{CD}_2\text{Cl}_2$ , 100.6 MHz):  $\delta$  216.15 (carbene C), 171.56 (C=O), 141.13 (Mes p-C), 135.10 (Mes o-C), 134.54 (Mes i-C), 130.65 (Mes m-CH), 85.53 (carborane  $\underline{\text{C}}^i\text{Pr}$ ), 83.98 (carborane  $\underline{\text{C}}\text{Cu}$ ), 52.31 (backbone  $\underline{\text{C}}(\text{CH}_3)_2$ ), 38.06 (carborane  $^i\text{Pr}$  CH), 24.96 (backbone  $\text{C}(\underline{\text{C}}\text{H}_3)_2$ ), 24.75 (carborane  $^i\text{Pr}$   $\text{CH}_3$ ), 21.26 (Mes p- $\text{CH}_3$ ), 18.31 (Mes o- $\text{CH}_3$ ).

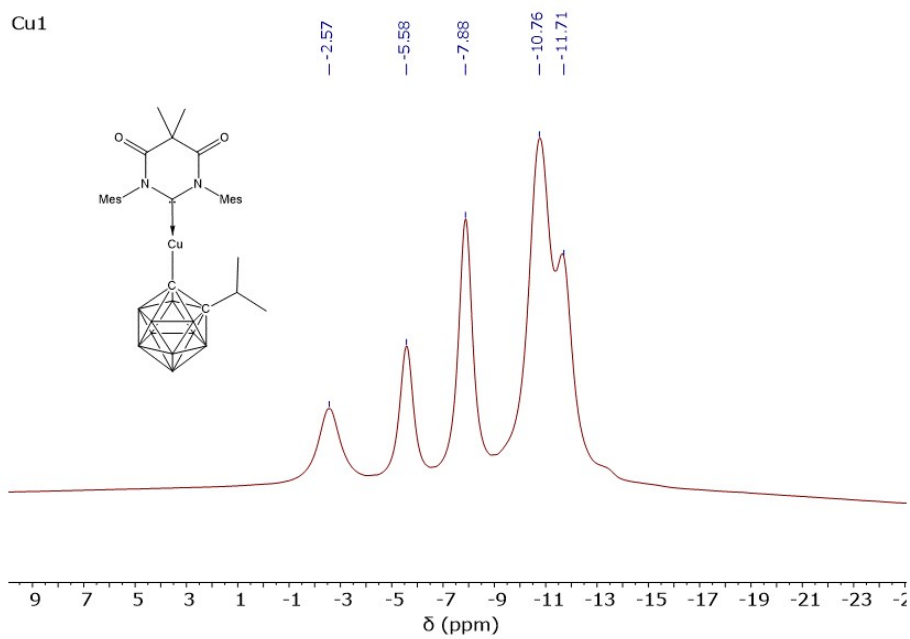
HRMS:  $\text{C}_{29}\text{H}_{45}\text{B}_{10}\text{N}_2\text{O}_2\text{Cu}$  theoretical  $[\text{M}+\text{H}]^+$ : 626.3843; found (APCI(ASAP)): 626.3839.

Anal. Calcd. For  $\text{C}_{29}\text{H}_{46}\text{B}_{10}\text{N}_2\text{O}_2\text{Cu}$ : C 55.61, H 7.40, N 4.47. Found: C 55.78, H 7.19, N 4.63.

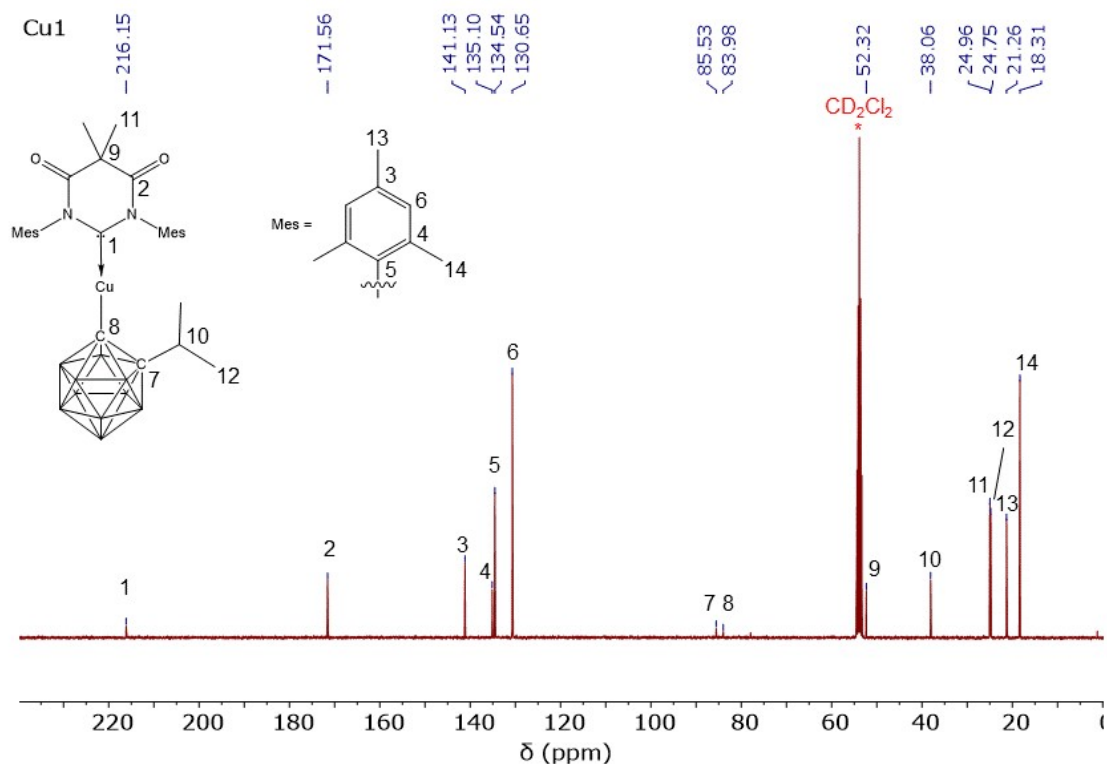


**Cu1  $^1H$  NMR (400 MHz,  $CD_2Cl_2$ )**

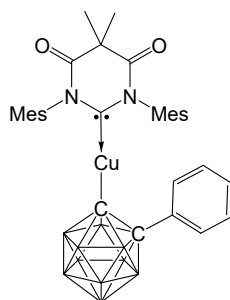
**Cu1  $^{11}B\{1H\}$  NMR (128.4 MHz,  $CD_2Cl_2$ )**



## Cu1 $^{13}\text{C}\{1\text{H}\}$ NMR (100.6 MHz, $\text{CD}_2\text{Cl}_2$ )



## Synthesis of (MesDAC)Cu(Ph-carboranyl) Cu2



A solution of 1-Li-2-Ph-1,2- $\text{C}_2\text{B}_{10}\text{H}_{10}$  (0.36 mmol) in THF (5 mL), prepared from 1-Ph-1,2- $\text{C}_2\text{B}_{10}\text{H}_{11}$  (80 mg, 0.36 mmol) and  $n\text{BuLi}$  (0.16 mL, 0.40 mmol), was cooled to  $-78^\circ\text{C}$  and a solution of  $[(\text{MesDAC})\text{CuCl}]_2$  (160 mg, 0.17 mmol) in THF (10 mL) was slowly added. The mixture was slowly warmed to room temperature and stirred overnight. The red mixture was evaporated to dryness, taken up in  $\text{CH}_2\text{Cl}_2$  and filtered through a short pad of celite and silica. The eluent was concentrated and purified by column chromatography (silica, 1:1



CH<sub>2</sub>Cl<sub>2</sub>/hexane) to give (MesDAC)Cu(Ph-carboranyl) as a yellow solid (42 mg, 0.06 mmol, 19%). Diffraction-quality crystals were grown by slow evaporation of a concentrated CH<sub>2</sub>Cl<sub>2</sub>/hexane solution.

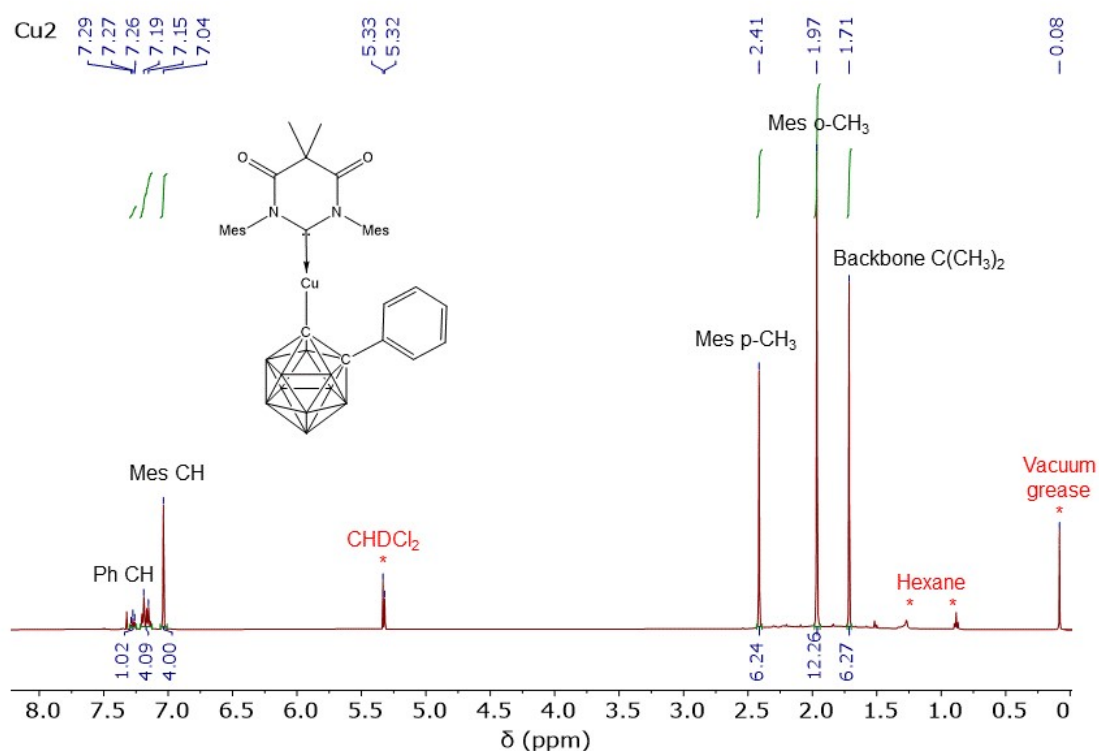
<sup>1</sup>H NMR (CD<sub>2</sub>Cl<sub>2</sub>, 400 MHz): δ 7.28 (t, *J* = 7.1 Hz, 1H, Ph *p*-CH), 7.17 (m, 4H, Ph *o*/*m*-CH), 7.04 (s, 4H, Mes CH), 2.8-0.8 (br m, 10H, BH envelope), 2.41 (s, 6H, Mes *p*-CH<sub>3</sub>), 1.96 (s, 12H, Mes *o*-CH<sub>3</sub>), 1.71 (s, 6H, backbone C(CH<sub>3</sub>)<sub>2</sub>).

<sup>11</sup>B{<sup>1</sup>H} NMR (CD<sub>2</sub>Cl<sub>2</sub>, 128.4 MHz): δ -1.5, -4.8, -7.5, -9.6, -10.8 (shoulder).

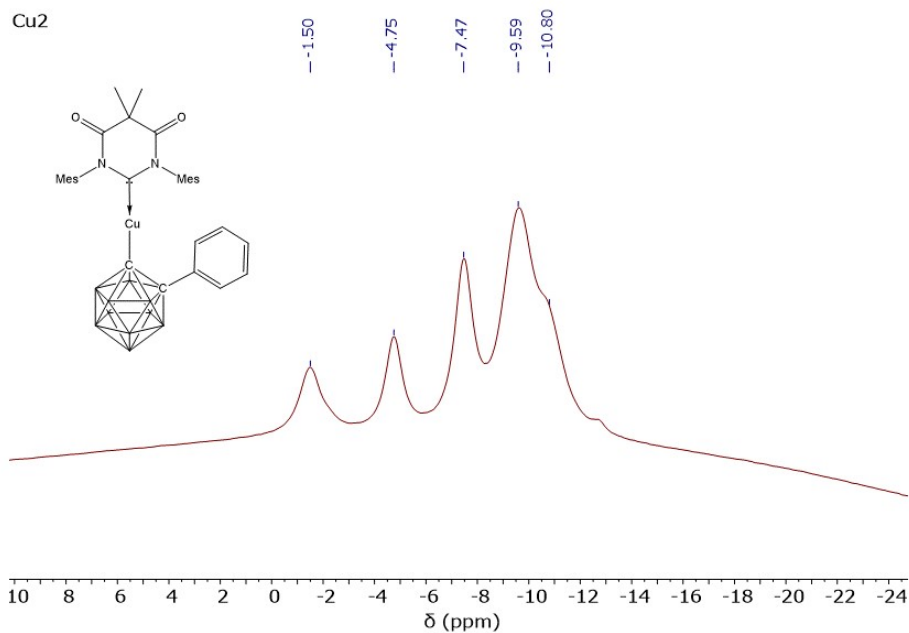
<sup>13</sup>C{<sup>1</sup>H} NMR (CD<sub>2</sub>Cl<sub>2</sub>, 100.6 MHz): δ 215.73\* (carbene C), 171.46 (C=O), 140.97 (Mes *p*-C), 138.86 (Ph *i*-C), 135.12 (Mes *o*-C), 134.34 (Mes *i*-C), 130.54 (Mes *m*-CH), 128.97 (Ph CH), 128.89 (Ph CH), 128.21 (Ph CH), 52.20 (backbone C(CH<sub>3</sub>)<sub>2</sub>), 24.92 (backbone C(CH<sub>3</sub>)<sub>2</sub>), 21.25 (Mes *p*-CH<sub>3</sub>), 18.23 (Mes *o*-CH<sub>3</sub>).

HRMS: C<sub>32</sub>H<sub>43</sub>B<sub>10</sub>N<sub>2</sub>O<sub>2</sub>Cu theoretical [M+H]<sup>+</sup>: 660.3694; found (APCI(ASAP)): 660.3684.

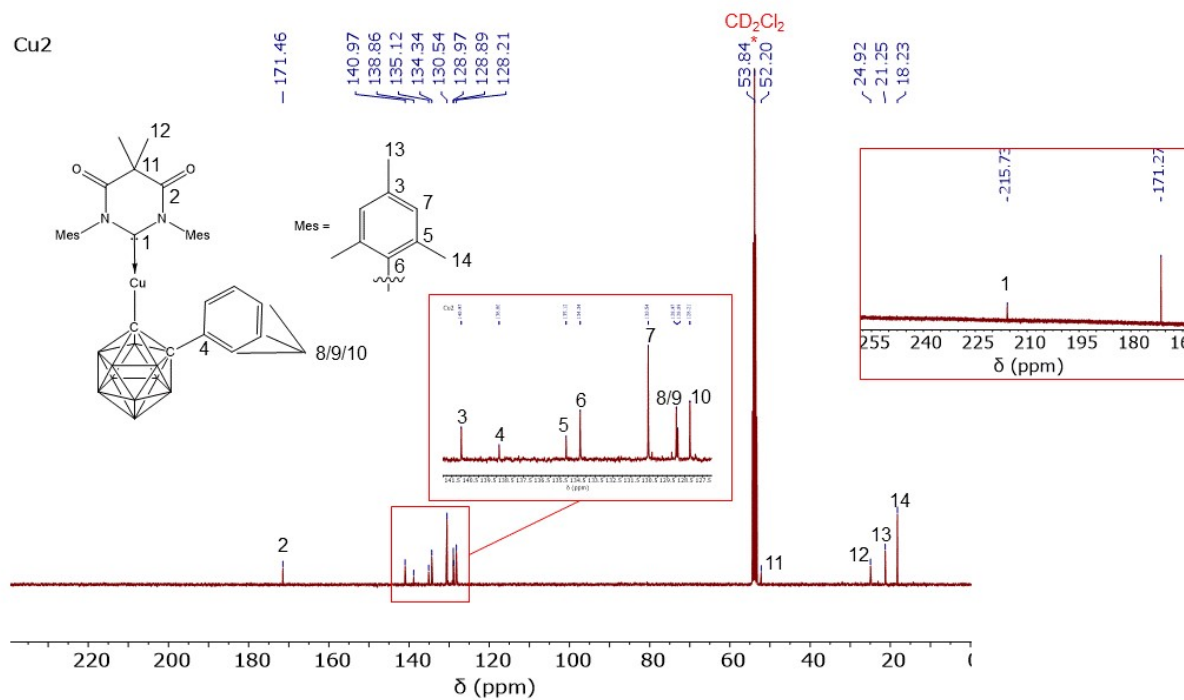
### Cu2 <sup>1</sup>H NMR (400 MHz, CD<sub>2</sub>Cl<sub>2</sub>)



**Cu2  $^{11}\text{B}\{1\text{H}\}$  NMR (128.4 MHz,  $\text{CD}_2\text{Cl}_2$ )**



**Cu2  $^{13}\text{C}\{1\text{H}\}$  NMR (100.6 MHz,  $\text{CD}_2\text{Cl}_2$ ; right insert 175 MHz,  $\text{CD}_2\text{Cl}_2$ )**





## Thermogravimetric Analysis.

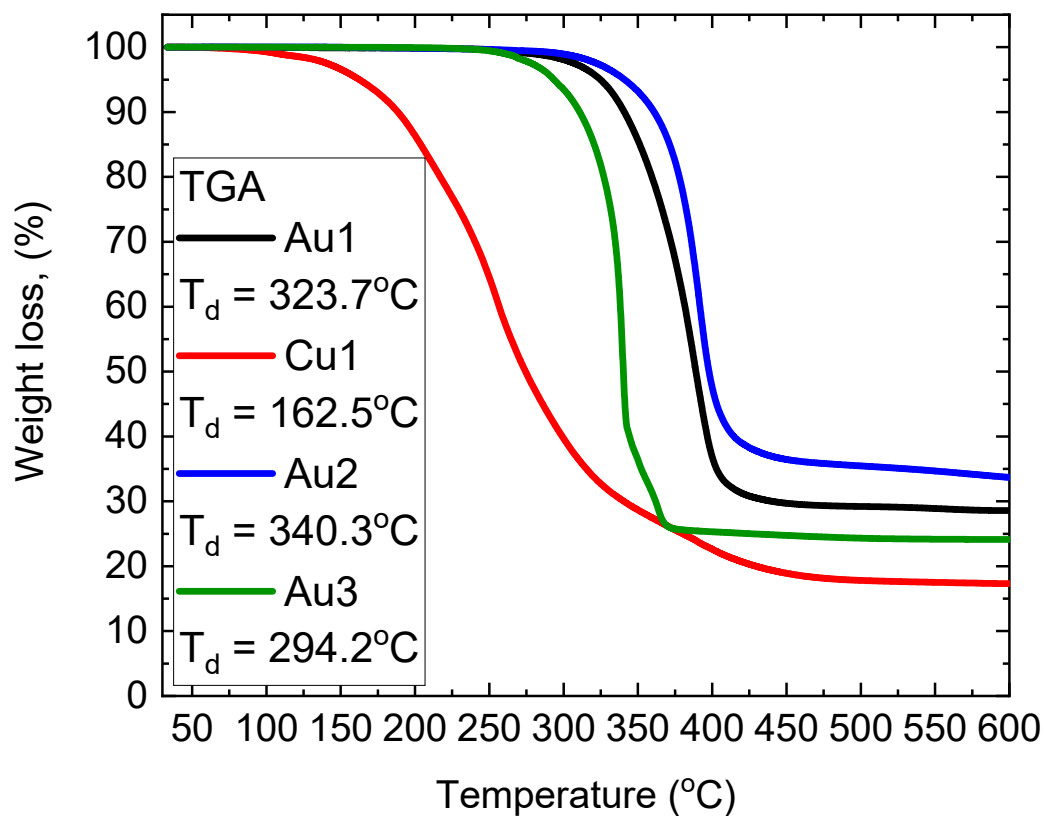


**Figure S1.** TGA curves for copper and gold complexes **Au1-Au3** and **Cu1**. Decomposition temperature ( $T_d$ ) indicates the temperature at 5% weight loss.

## Single Crystal X-ray Crystallography.

All crystals were mounted in oil on a MiTeGen loop and fixed on the diffractometer in a cold nitrogen stream. Data were collected using dual wavelength Rigaku FR-X rotating anode diffractometer using  $\text{CuK}\alpha$  ( $\lambda = 1.54146 \text{ \AA}$ ) radiation, equipped with an AFC-11 4-circle kappa goniometer, VariMAX<sup>TM</sup> microfocus optics, a Hypix-6000HE detector and an Oxford Cryosystems 800 plus nitrogen flow gas system, at a temperature of 100K. Data were collected and reduced using CrysAlisPro v42.<sup>5,6</sup> The structure was solved by intrinsic phasing or direct method and refined by the full-matrix least-squares against F<sup>2</sup> in an anisotropic (for non-hydrogen atoms) approximation. Absorption correction was performed using empirical methods (SCALE3 ABSPACK) based upon symmetry-equivalent reflections combined with measurements at different azimuthal angles. All hydrogen atom positions were refined in isotropic approximation in a “riding” model with the  $U_{\text{iso}}(\text{H})$  parameters equal to  $1.2 U_{\text{eq}}(\text{C}_i)$ , for methyl groups equal to  $1.5 U_{\text{eq}}(\text{C}_{ii})$ , where  $U(\text{C}_i)$  and  $U(\text{C}_{ii})$  are respectively the equivalent thermal parameters of the carbon atoms to which the corresponding H atoms are bonded. All calculations were performed using the SHELXTL software.<sup>7</sup> OLEX2 software was used as graphical user interface.<sup>8</sup>

The principal crystallographic data and refinement parameters are listed below:

Complex **Au1**, CCDC number 2280891,  $\text{C}_{29}\text{H}_{45}\text{AuB}_{10}\text{N}_2\text{O}_2$  ( $M = 758.73 \text{ g/mol}$ ): monoclinic, space group  $\text{P}2_1/\text{n}$  (no. 14),  $a = 11.1127(4) \text{ \AA}$ ,  $b = 26.6626(9) \text{ \AA}$ ,  $c = 11.4450(4) \text{ \AA}$ ,  $\beta = 98.835(3)^\circ$ ,  $V = 3350.8(2) \text{ \AA}^3$ ,  $Z = 4$ ,  $T = 100.00(11) \text{ K}$ ,  $\mu(\text{Mo K}\alpha) = 4.421 \text{ mm}^{-1}$ ,  $D_{\text{calc}} = 1.504 \text{ g/cm}^3$ , 44387 reflections measured ( $3.054^\circ \leq 2\Theta \leq 61.764^\circ$ ), 8795 unique ( $R_{\text{int}} = 0.0398$ ,  $R_{\text{sigma}} = 0.0360$ ) which were used in all calculations. The final  $R_1$  was 0.0249 ( $I > 2\sigma(I)$ ) and  $wR_2$  was 0.0487 (all data).

Complex **Au2**, CCDC number 2280892, colorless block,  $\text{C}_{32}\text{H}_{43}\text{AuB}_{10}\text{N}_2\text{O}_2$  ( $M = 792.75 \text{ g/mol}$ ): monoclinic, space group  $\text{P}2_1/\text{c}$  (no. 14),  $a = 10.53700(10) \text{ \AA}$ ,  $b = 18.0731(2) \text{ \AA}$ ,  $c = 20.1419(2) \text{ \AA}$ ,  $\beta = 95.8610(10)^\circ$ ,  $V = 3815.70(7) \text{ \AA}^3$ ,  $Z = 4$ ,  $T = 100.00(10) \text{ K}$ ,  $\mu(\text{Cu K}\alpha) = 7.461 \text{ mm}^{-1}$ ,  $D_{\text{calc}} = 1.380 \text{ g/cm}^3$ , 49649 reflections measured ( $8.436^\circ \leq 2\Theta \leq 151.704^\circ$ ), 7884 unique ( $R_{\text{int}} = 0.0364$ ,  $R_{\text{sigma}} = 0.0246$ ) which were used in all calculations. The final  $R_1$  was 0.0266 ( $I > 2\sigma(I)$ ) and  $wR_2$  was 0.0675 (all data).

Complex **Au3**, CCDC number 2280893, colorless block,  $\text{C}_{35}\text{H}_{57}\text{AuB}_{10}\text{N}_2\text{O}_2$  ( $M = 842.89 \text{ g/mol}$ ): monoclinic, space group  $\text{P}2_1/\text{n}$  (no. 14),  $a = 11.48602(12) \text{ \AA}$ ,  $b = 19.7064(2) \text{ \AA}$ ,  $c = 17.35568(19) \text{ \AA}$ ,  $\beta = 93.0324(10)^\circ$ ,  $V = 3922.93(7) \text{ \AA}^3$ ,  $Z = 4$ ,  $T = 100.00(13) \text{ K}$ ,  $\mu(\text{Cu K}\alpha) = 7.286 \text{ mm}^{-1}$ ,  $D_{\text{calc}} = 1.427 \text{ g/cm}^3$ , 23741 reflections measured ( $6.792^\circ \leq 2\Theta \leq 151.916^\circ$ ), 7971

unique ( $R_{\text{int}} = 0.0214$ ,  $R_{\text{sigma}} = 0.0226$ ) which were used in all calculations. The final  $R_1$  was 0.0230 ( $I > 2\sigma(I)$ ) and  $wR_2$  was 0.0635 (all data).

Complex **Cu1**, CCDC number 2280894, yellow block,  $\text{C}_{29}\text{H}_{45}\text{B}_{10}\text{CuN}_2\text{O}_2$  ( $M = 625.31$  g/mol): monoclinic, space group  $P2_1/n$  (no. 14),  $a = 10.9247(2)$  Å,  $b = 26.7491(4)$  Å,  $c = 11.4847(2)$  Å,  $\beta = 97.260(2)^\circ$ ,  $V = 3329.22(10)$  Å<sup>3</sup>,  $Z = 4$ ,  $T = 100.00(10)$  K,  $\mu(\text{Mo K}\alpha) = 0.686$  mm<sup>-1</sup>,  $D_{\text{calc}} = 1.248$  g/cm<sup>3</sup>, 27413 reflections measured ( $7.066^\circ \leq 2\Theta \leq 58.182^\circ$ ), 7806 unique ( $R_{\text{int}} = 0.0379$ ,  $R_{\text{sigma}} = 0.0424$ ) which were used in all calculations. The final  $R_1$  was 0.0390 ( $I > 2\sigma(I)$ ) and  $wR_2$  was 0.0982 (all data).

Complex **Cu2**, CCDC number 2280895, yellow block,  $\text{C}_{35}\text{H}_{50}\text{B}_{10}\text{CuN}_2\text{O}_2$  ( $M = 702.41$  g/mol): monoclinic, space group  $P2_1/c$  (no. 14),  $a = 10.63269(10)$  Å,  $b = 18.25848(15)$  Å,  $c = 19.63777(18)$  Å,  $\beta = 96.5490(8)^\circ$ ,  $V = 3787.53(6)$  Å<sup>3</sup>,  $Z = 4$ ,  $T = 99.99(17)$  K,  $\mu(\text{Cu K}\alpha) = 1.058$  mm<sup>-1</sup>,  $D_{\text{calc}} = 1.232$  g/cm<sup>3</sup>, 47417 reflections measured ( $6.63^\circ \leq 2\Theta \leq 152.178^\circ$ ), 7822 unique ( $R_{\text{int}} = 0.0398$ ,  $R_{\text{sigma}} = 0.0289$ ) which were used in all calculations. The final  $R_1$  was 0.0390 ( $I > 2\sigma(I)$ ) and  $wR_2$  was 0.1063 (all data).

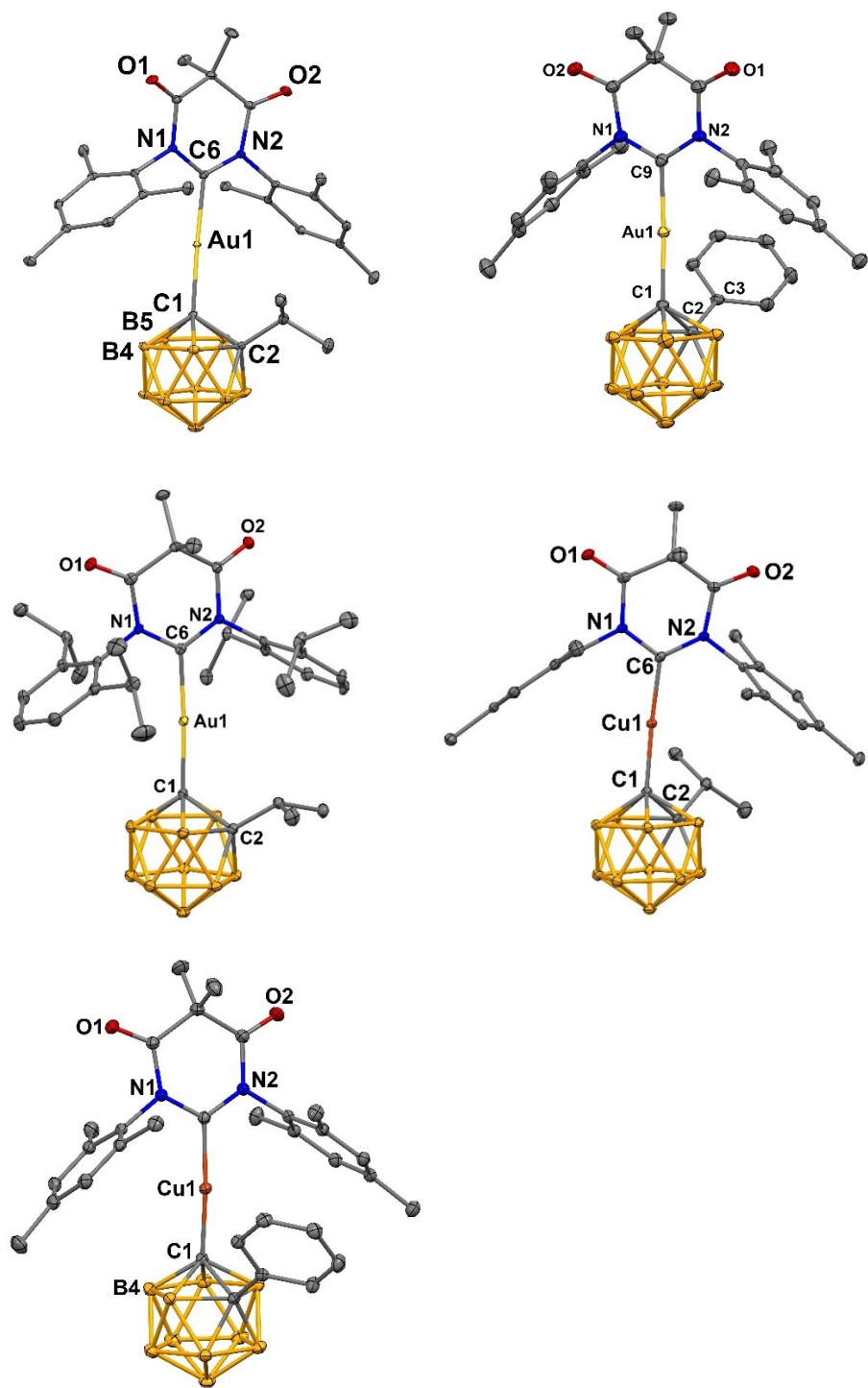
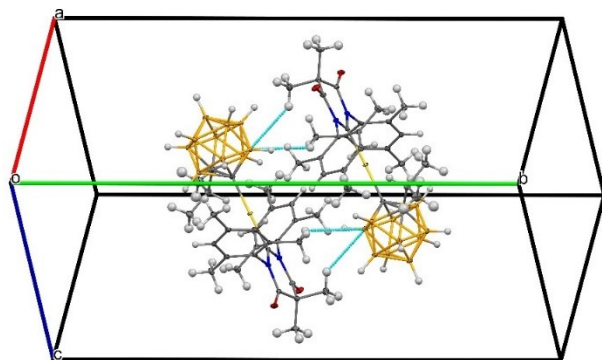


**Figure S2.** Crystal structures of carbene-metal-carborane (CMC) complexes (top left) **Au1**, (top right) **Au2** (middle left) **Au3**, (middle right) **Cu1** and (bottom left) **Cu2** at 100 K, showing the conformations adopted by the substituted carborane ligands. Ellipsoids are shown at the 50% level. Hydrogen atoms are omitted for clarity. For structural parameters, see Table S1.

**Table S1.** Selected bond lengths [ $\text{\AA}$ ] and angles [ $^\circ$ ] of copper and gold carborane complexes.

	M–C <sub>carborane</sub> , $\text{\AA}$	M–C <sub>DAC</sub> , $\text{\AA}$	C1 $\cdots$ C6, $\text{\AA}$	angle, $^\circ$ C1–M–C6	torsion angle, $^\circ$ N2–C6–C1–C2
<b>Au1</b>	2.044(2)	2.016(2)	4.059(2)	176.25(9)	45.0(2)
<b>Au2</b>	2.042(3)	2.015(3)	4.055(3)	175.89(11)	78.7(2)
<b>Au3</b>	2.050(2)	2.019(2)	4.067(2)	176.81(9)	39.0(1)
<b>Cu1</b>	1.919(2)	1.895(2)	3.813(2)	176.51(8)	42.9(2)
<b>Cu2</b>	1.912(2)	1.887(2)	3.791(3)	171.75(7)	76.8(2)

**Complex Au1**



**Complex Cu2**

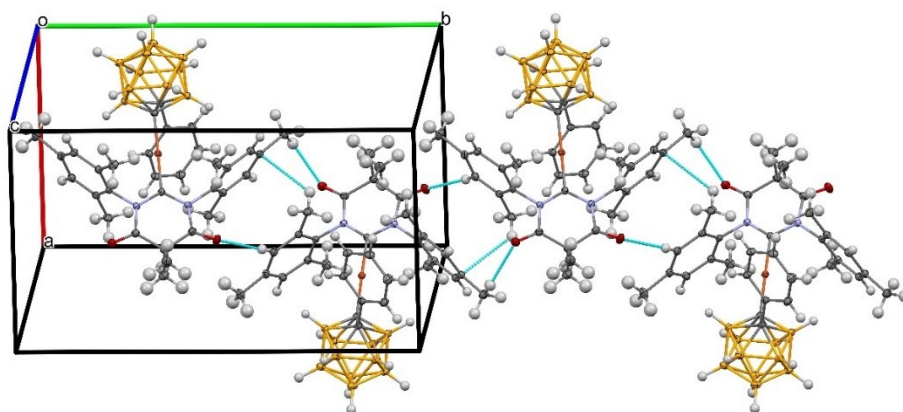


**Figure S3.** Head-to-tail orientation of the molecules of complex **Au1** (top) and zig-zag chains for copper complex **Cu2** (bottom) in the unit cell.



## Cyclic Voltammetry.

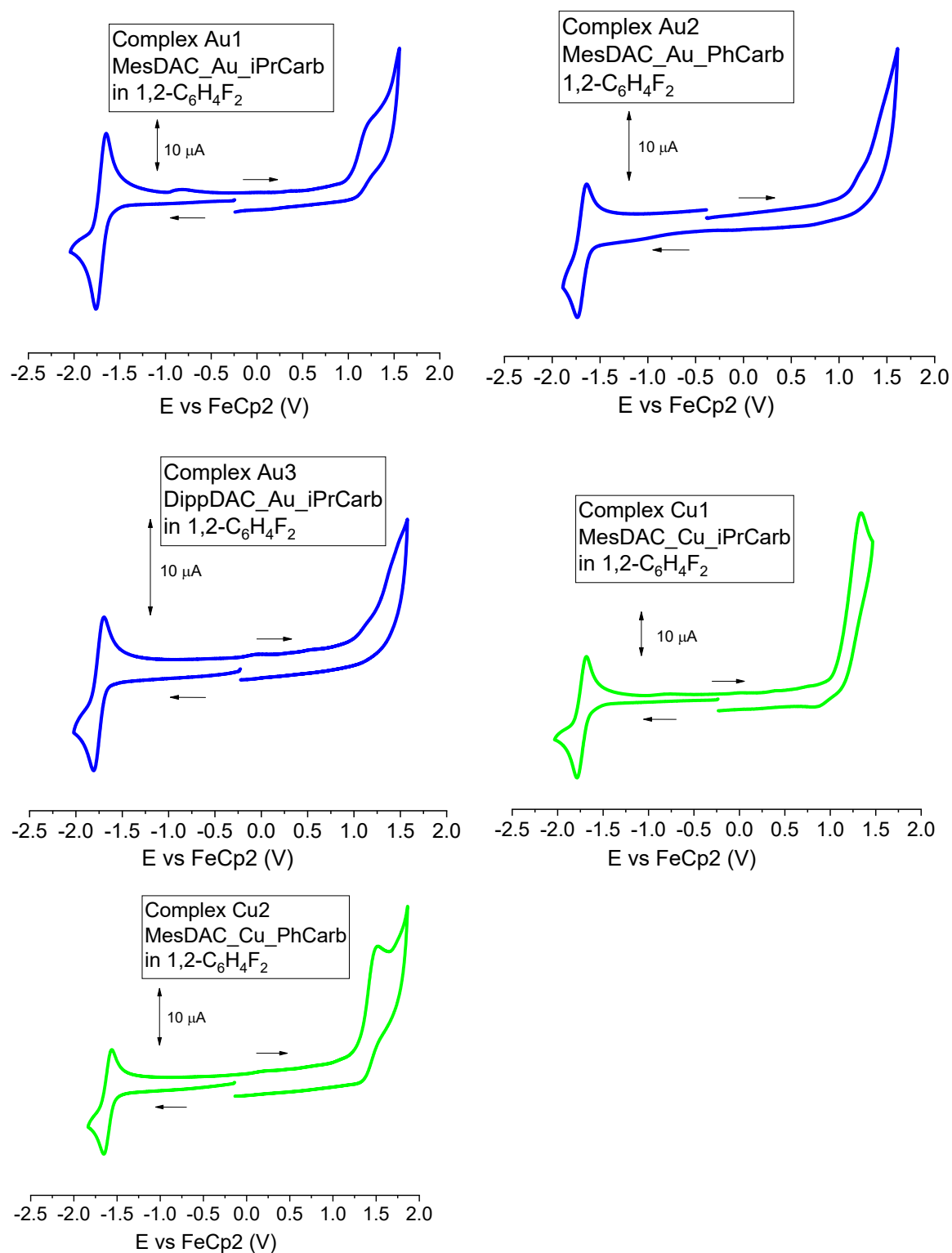


**Figure S4.** Full range cyclic voltammogram for (top left) **Au1**, (top right) **Au2**, (middle left) **Au3**, (middle right) **Cu1** and (bottom left) **Cu2**. Recorded using a glassy carbon electrode in THF solution (1.4 mM) with  $[n\text{-Bu}_4\text{N}]\text{PF}_6$  as supporting electrolyte (0.13 M), scan rate  $0.1 \text{ V s}^{-1}$ .

**Table S2.** Formal electrode potentials (peak position  $E_p$  for irreversible and  $E_{1/2}$  for quasi-reversible processes (\*),  $V$ , vs. FeCp<sub>2</sub>), onset potentials ( $E$ ,  $V$ , vs. FeCp<sub>2</sub>), peak-to-peak separation in parentheses for quasi-reversible processes ( $\Delta E_p$  in mV),  $E_{HOMO}/E_{LUMO}$  (eV) and band gap values ( $\Delta E$ , eV) for the redox changes exhibited by copper and gold complexes.<sup>a</sup>

Complex	Reduction		$E_{LUMO}$ eV	Oxidation		$E_{HOMO}$ eV	$\Delta E$ eV
	$E_{1/2}$	$E_{onset\ red}$		$E_p$	$E_{onset\ ox}$		
<b>Au1</b>	-1.76 (109)	-1.62	-3.77	+1.24	+1.03	-6.42	2.65
<b>Au2</b>	-1.74 (95)	-1.61	-3.78	+1.49	+1.21	-6.60	2.82
<b>Au3</b>	-1.81 (112)	-1.68	-3.71	+1.46	+1.14	-6.53	2.82
<b>Cu1</b>	-1.79 (105)	-1.66	-3.73	+1.33	+1.09	-6.48	2.75
<b>Cu2</b>	-1.65 (92)	-1.53	-3.86	+1.51	+1.32	-6.71	2.85

<sup>a</sup> In 1,2-difluorobenzene solution, recorded using a glassy carbon electrode, concentration 1.4 mM, supporting electrolyte [*n*-Bu<sub>4</sub>N][PF<sub>6</sub>] (0.13 M), measured at 0.1 V s<sup>-1</sup>.  $E_{HOMO} = -(E_{onset\ ox\ Fc/Fc^+} + 5.39)$  eV;  $E_{LUMO} = -(E_{onset\ red\ Fc/Fc^+} + 5.39)$  eV (*Adv. Mater.* **2011**, *23*, 2367–2371).

## **Photophysical Characterisation.**

### **Experimental Methods for Spectroscopy**

#### *Sample Preparation*

Samples for photophysics were made from powders stored in a glovebox.

#### *Photoluminescence Quantum Yield*

. Photoluminescence quantum yields were recorded in air for solid samples using a Hamamatsu Quantaurus-QY C11347-11.

#### *Steady-state Photoluminescence*

Steady-state PL spectra were recorded using an Edinburgh Instruments FLS980 spectrofluorimeter. The light source was a monochromated Xenon arc lamp; excitation wavelength varied. Samples were measured in air or under flowing nitrogen, at room temperature.

#### *UV-Vis Absorption*

UV-Vis spectra were measured using a Varian Cary 5000 UV-Vis-NIR spectrometer and Shimadzu UV-3600 Plus UV-VIS-NIR spectrophotometer. The spectrometer has a PMT detector for wavelength ranges from UV to visible, as well as InGaAs and PbS detectors for NIR. The light source used was a deuterium lamp for wavelengths less than 280nm and a tungsten halogen lamp for higher wavelengths.

## UV-Vis and Photoluminescence Spectra:

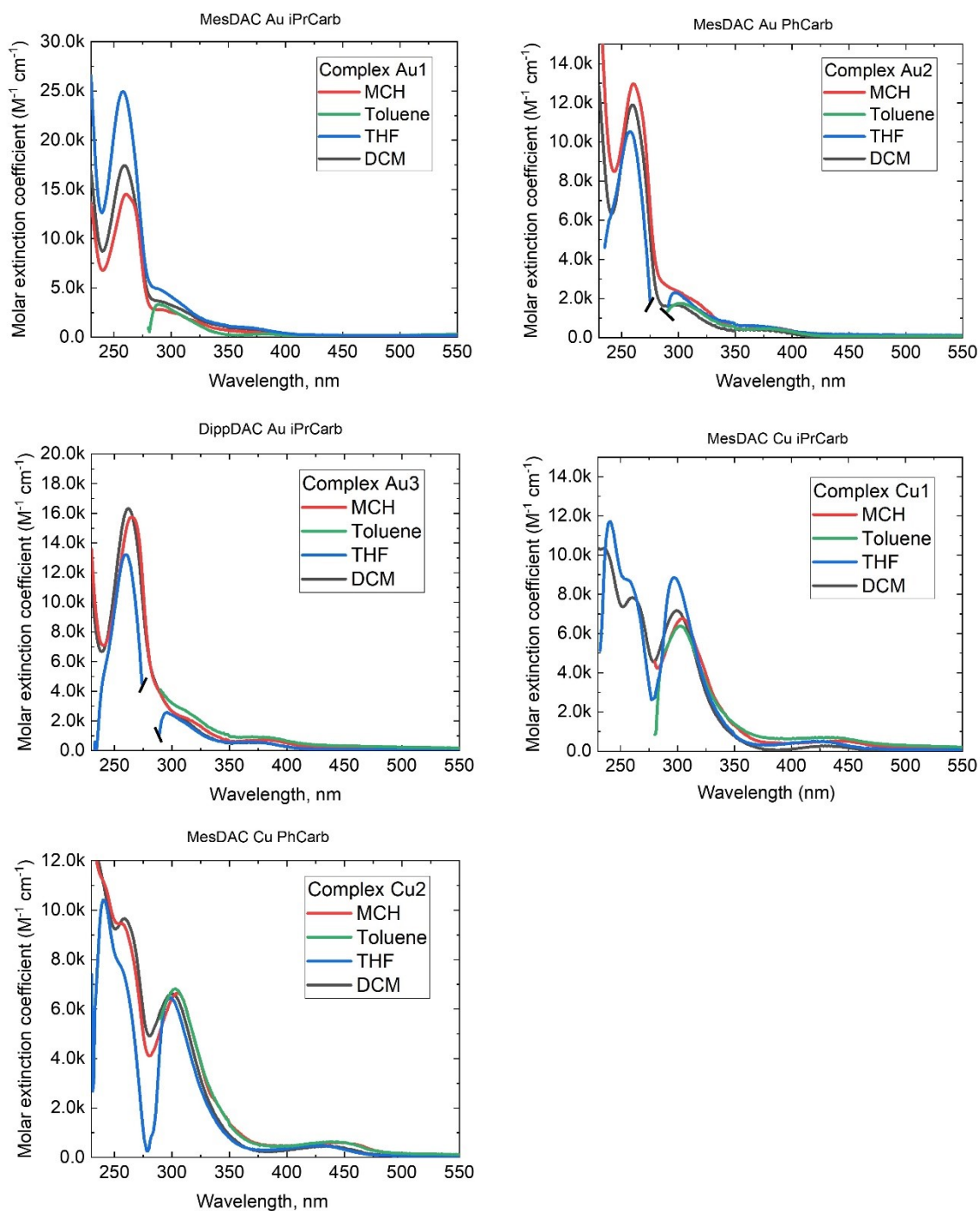


**Figure S5a.** UV-Vis spectra for (top left) **Au1**, (top right) **Au2**, (middle left) **Au3**, (middle right) **Cu1** and (bottom left) **Cu2** at 295 K in various solvents where MCH = methylcyclohexane, THF = tetrahydrofuran (high energy part of the UV-vis profile from 275 to 290 nm was truncated for **Au2** and **Au3** due to strong solvent absorption), DCM = dichloromethane.

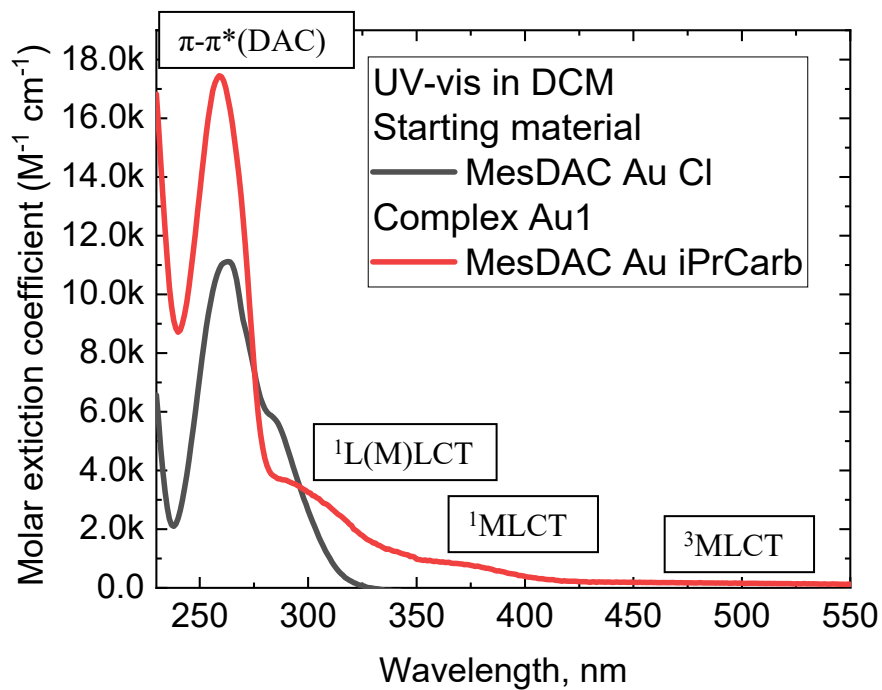


**Figure S5b.** UV-Vis spectra for starting material (MesDAC)AuCl and **Au1** in DCM at 295K.

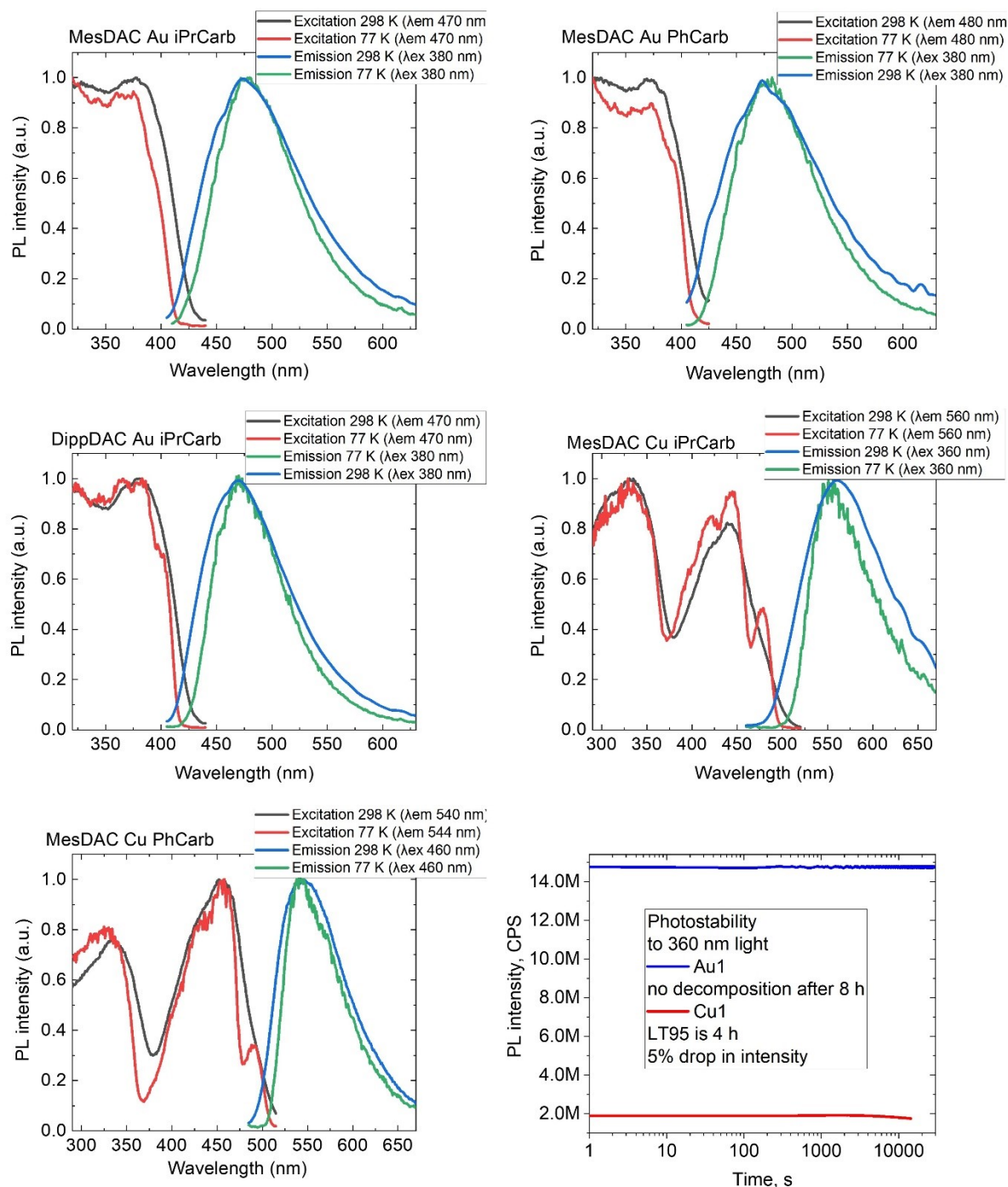


**Figure S6.** Photoluminescence spectra for (top left) **Au1**, (top right) **Au2**, (middle left) **Au3**, (middle right) **Cu1** and (bottom left) **Cu2** at 295 and 77K in crystalline state. Photostability for complexes **Au1** and **Cu1** under  $N_2$  atmosphere and constant exposure to the UV-light at 360 nm (top, right).

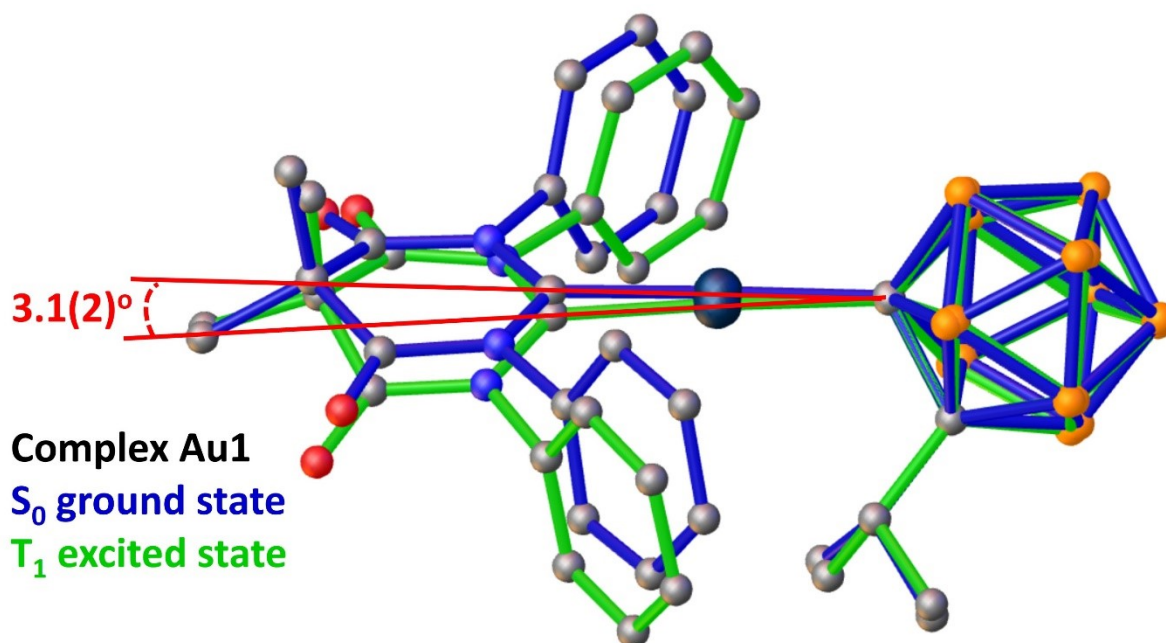
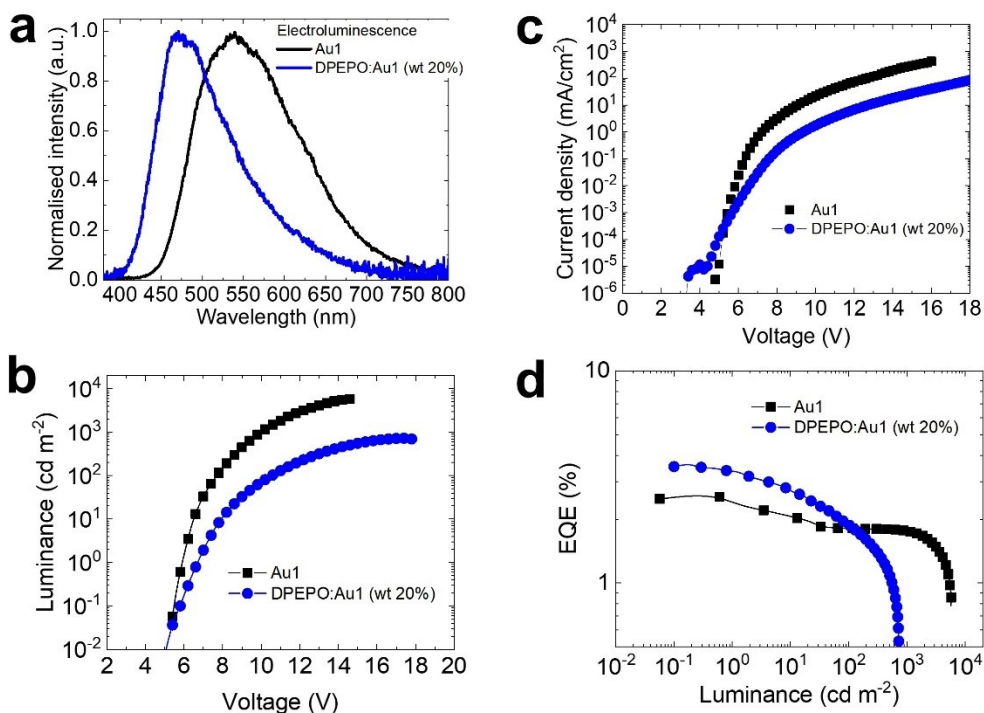


**Figure S7.** Superposition of the ground state  $S_0$  (single crystal X-ray) and excited triplet state  $T_1$  geometries for complex **Au1** (overlay via C1, C2 and Au1 atoms) determined by theoretical calculations where angle is Au1( $S_0$  geometry)–C1–Au1 ( $T_1$  geometry).

### Device fabrication and characterization

For the fabrication of OLED devices, ITO coated substrates ( $\sim 15 \Omega/\text{cm}^2$ ) were cleaned with acetone and isopropyl alcohol, and then  $\text{O}_2$  plasma treatment was applied to align the energy level with a hole transporting layer. All layers, including organic layers and a LiF/aluminium cathode, were thermally deposited in high vacuum ( $\sim 10^{-7}$  torr).

The performance of the OLED devices was measured by a Keithley 2635 source-meter and a calibrated Si photodiode. The EL spectra were recorded by an Ocean Optics Flame spectrometer.



ITO
TAPC 30 nm
TCTA 10 nm
mCP 10 nm
EML 20 nm
DPEPO 10 nm
TPBi 35 nm
LiF 1 nm / Al 100 nm

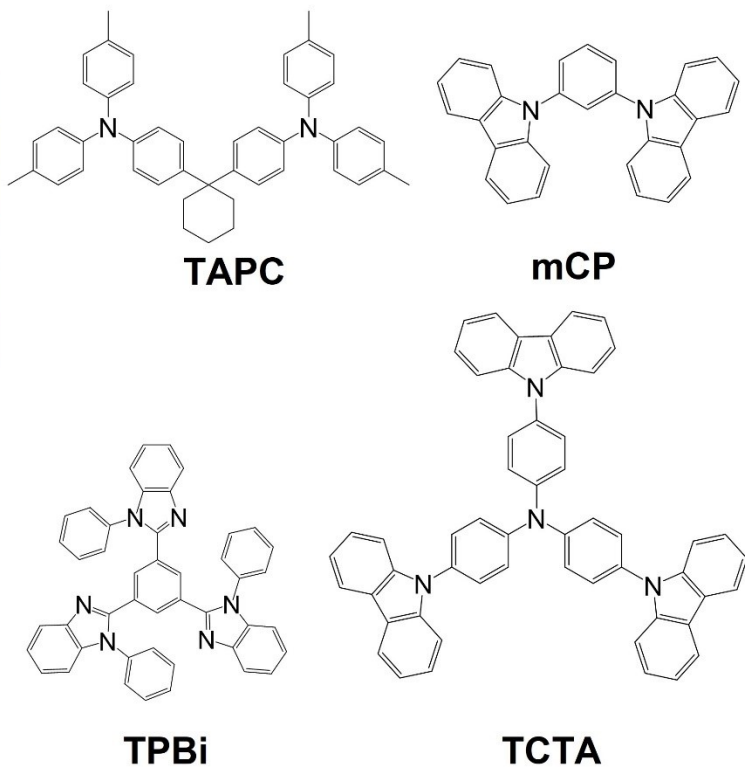


**Figure S8.** (a) Electroluminescence spectra of **Au1** in neat OLED and doped in DPEPO host with 20% weight concentration; (b) current density-voltage plot; (c) luminance-voltage plot; (d) EQE versus luminance. The OLED device stack and the molecular structure of the components are shown at the bottom.



**Table S3.** Performance data of vapor-deposited OLEDs.

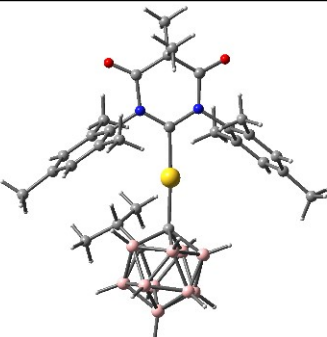
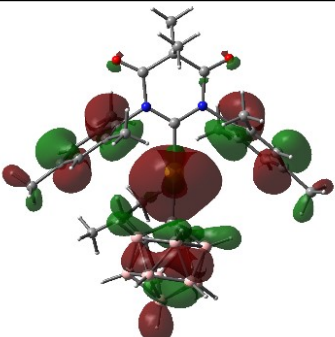
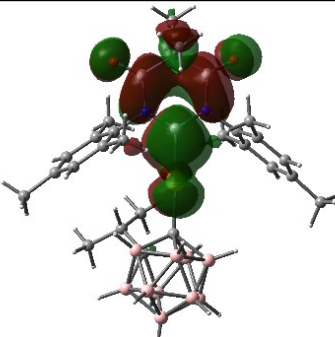
Dopant	$V_{ON}$ [V] <sup>a</sup>	EQE (%)		EL (nm)	Luminance cd m <sup>-2</sup>	CIE (x,y) <sup>b</sup>
		max	100 cd m <sup>-2</sup>			
Neat Au1	5.5	2.6	1.8	540	5770	0.378, 0.503
DPEPO:Au1	5.8	3.6	1.8	471	726	0.225, 0.306

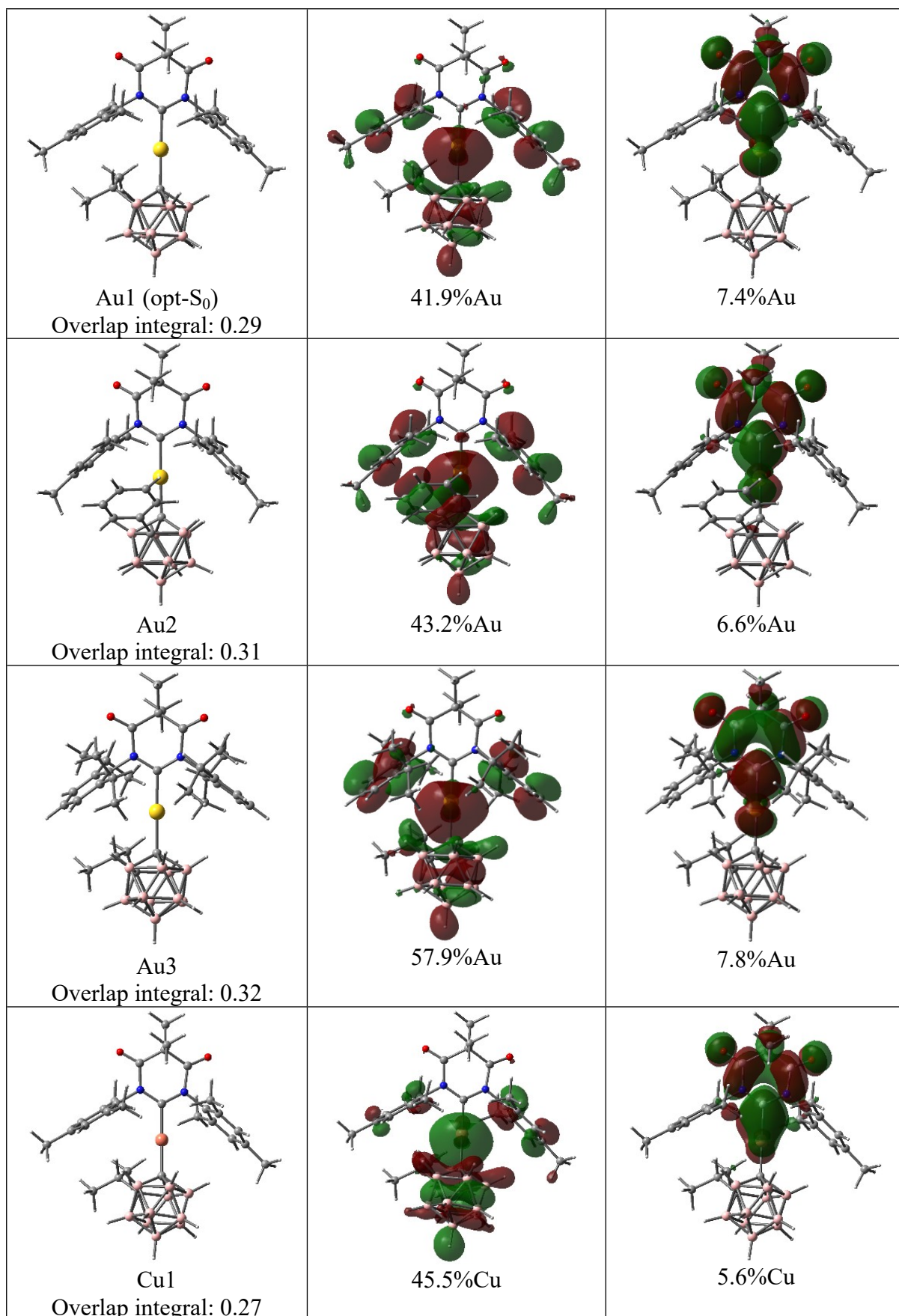
<sup>a</sup> At brightness 0.1 cd m<sup>-2</sup>; <sup>b</sup> Commission Internationale de l'Éclairage (CIE) color coordinates

### Computational details

The ground states of the complexes were studied by density functional theory (DFT) and the excited states by time-dependent DFT (TD-DFT) using the Tamm-Dancoff approximation, as implemented in Gaussian 16.<sup>9,10,11</sup> Calculations were carried out by the global hybrid MN15 functional of the Minnesota series in combination with the def2-TZVP basis set,<sup>12,13</sup> employing relativistic effective core potential of 60 electrons for description of the core electrons of Au.<sup>14</sup> This methodology has been employed in several papers dealing with closely related complexes, in good agreement with experiments.<sup>15</sup> Orbital compositions were evaluated by Mulliken population analysis as implemented in Gaussian. Orbital overlaps were calculated using Multiwfn program.<sup>16</sup>

**Table S4.** HOMO and LUMO isosurface plots, HOMO-LUMO overlap integrals, and metal atom contributions to the orbitals in the optimized S<sub>0</sub> geometry, including crystal structure geometry for Au1.

	HOMO	LUMO
 Au1 (crystal) Overlap integral: 0.30	 41.8%Au	 7.4%Au



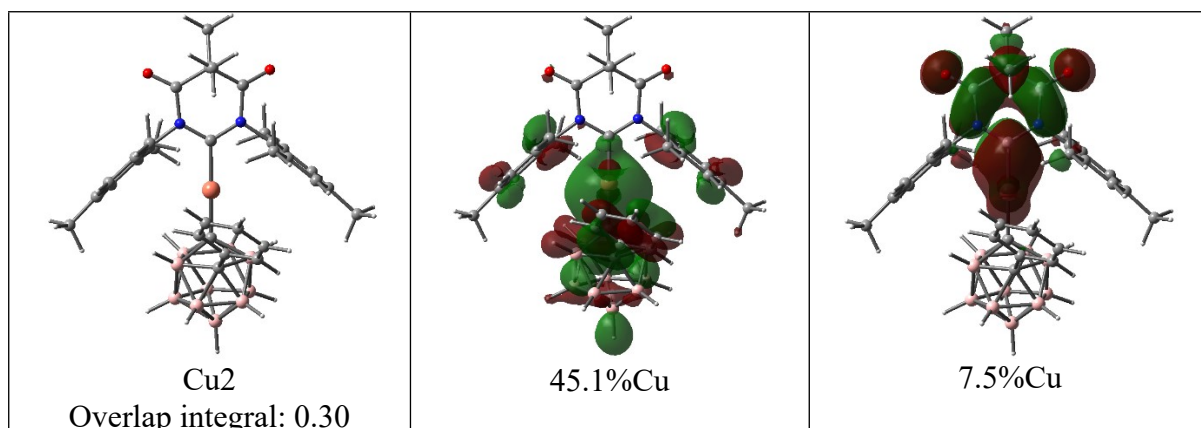


**Table S5.** M-C(Carborane) and M-C(DAC) bonds dissociation energies in the optimized  $S_0$  geometry.

	M-C(Carborane)		M-C(DAC)	
	kJ/mol	eV	kJ/mol	eV
Au1	452.7	4.69	333.8	3.46
Au2	457.7	4.74	335.5	3.48
Au3	462.4	4.79	339.8	3.52
Cu1	454.5	4.71	304.1	3.15
Cu2	455.9	4.73	298.0	3.09

**Table S6.** Dipole moments for  $S_0$  and lowest singlet vertical excitations in the optimized  $S_0$  geometry, including crystal structure geometry for Au1.

	$S_0$	$S_1@S_0$
Au1 (crystal)	 10.9D	 4.5D
Au1 (opt- $S_0$ )	 10.1D	 3.2D

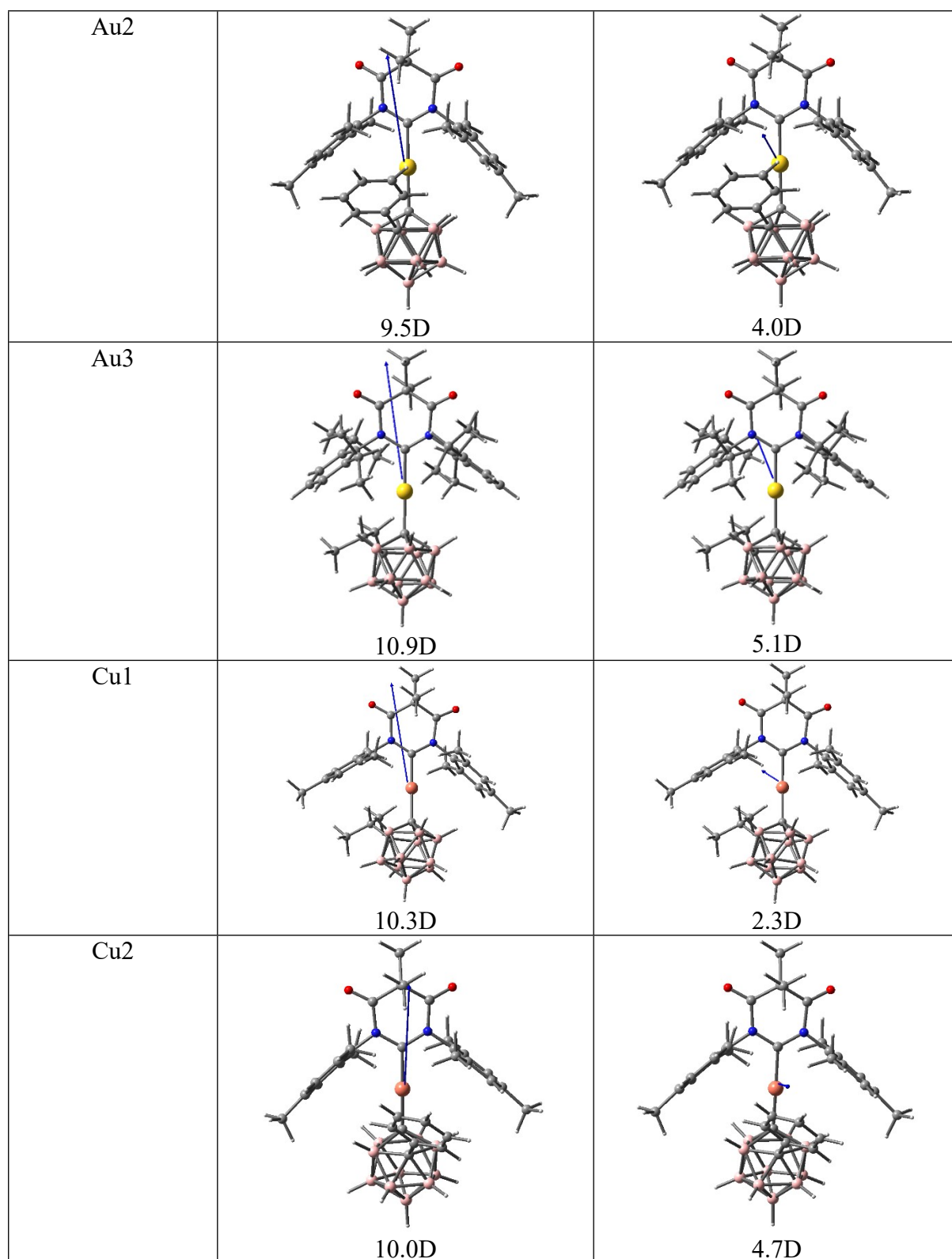


**Table S7.** Vertical excitations, their character, and  $S_0$ - $S_1$  oscillator strength coefficients.

	Excitation energy	Character	Oscillator strength
Au1 (crystal)	$S_1$ ( $^1LE(M+DAC)$ ): 3.32eV = 374nm	HOMO – LUMO	0.0033

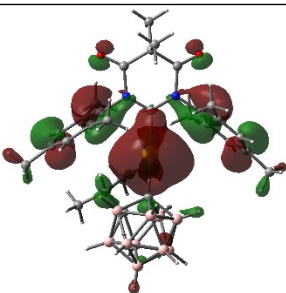
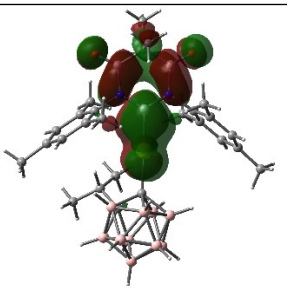
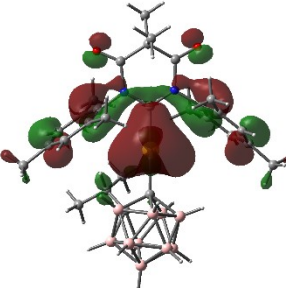
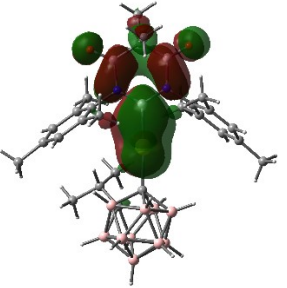
		(88%)	
	T <sub>1</sub> ( <sup>3</sup> LE(M+DAC)): 3.11eV = 398nm	HOMO – LUMO (74%)	
	T <sub>2</sub> (mixed <sup>3</sup> CT and <sup>3</sup> LE(DAC)): 3.70eV = 335nm	HOMO-1 – LUMO (39%)	
	T <sub>3</sub> ( <sup>3</sup> LE(M+DAC)): 3.85eV = 322nm	HOMO-1 – LUMO (45%) HOMO-4 – LUMO (35)	
Au2	S <sub>1</sub> (mixed <sup>1</sup> CT(M→DAC) and <sup>1</sup> LE(DAC)): 3.26eV = 381nm	HOMO – LUMO (89%)	0.0045
	T <sub>1</sub> (mixed <sup>3</sup> CT(M→DAC) and <sup>3</sup> LE(DAC)): 3.04eV = 408nm	HOMO – LUMO (78%)	
	T <sub>2</sub> (mixed <sup>3</sup> CT(Carb→DAC) and <sup>3</sup> LE(DAC)): 3.76eV = 330nm	HOMO-1 – LUMO (36%)	
	T <sub>3</sub> (mixed <sup>3</sup> CT(Carb→DAC) and <sup>3</sup> LE(DAC)): 3.79eV = 327nm	HOMO-1 – LUMO (44%)	
	T <sub>4</sub> ( <sup>3</sup> LE(DAC)): 3.96eV = 313nm	HOMO-3 – LUMO (17%)	
Au3	S <sub>1</sub> (mixed <sup>1</sup> CT(M→DAC) and <sup>1</sup> LE(DAC)): 3.25eV = 381nm	HOMO – LUMO (88%)	0.0052
	T <sub>1</sub> (mixed <sup>3</sup> CT(M→DAC) and <sup>3</sup> LE(DAC)): 3.03eV = 409nm	HOMO – LUMO (74%)	
	T <sub>2</sub> (mixed <sup>3</sup> CT(Carb→DAC) and <sup>3</sup> LE(DAC)): 3.68eV = 337nm	HOMO-3 – LUMO (41%) HOMO – LUMO (15%)	
	T <sub>3</sub> ( <sup>3</sup> LE(DAC)): 3.85eV = 322nm	HOMO-1 – LUMO (71%)	
Cu1	S <sub>1</sub> (mixed <sup>1</sup> CT and <sup>1</sup> LE(DAC)): 2.96eV = 419nm	HOMO – LUMO (82%)	0.0050
	T <sub>1</sub> ( <sup>3</sup> LE(M+DAC)): 2.64eV = 470nm	HOMO – LUMO (65%)	
	T <sub>2</sub> (mixed <sup>3</sup> CT and <sup>3</sup> LE(DAC)): 3.49eV = 356nm	HOMO-1 – LUMO (32%) HOMO – LUMO (19%)	
	T <sub>3</sub> ( <sup>3</sup> LE(M+DAC)): 3.82eV = 324nm	HOMO-1 – LUMO (34%) HOMO-3 – LUMO (28%)	
Cu2	S <sub>1</sub> (mixed <sup>1</sup> CT(M→DAC) and <sup>1</sup> LE(DAC)): 2.92eV = 425nm	HOMO – LUMO (85%)	0.0105
	T <sub>1</sub> (mixed <sup>3</sup> CT(M→DAC) and <sup>3</sup> LE(DAC)): 2.58eV = 480nm	HOMO – LUMO (70%)	
	T <sub>2</sub> (mixed <sup>3</sup> CT(Carb→DAC) and <sup>3</sup> LE(DAC)): 3.53eV = 351nm	HOMO – LUMO (14%) HOMO-5 – LUMO (13%)	

		HOMO-2 – LUMO (12%)	
	$T_3$ (mixed ${}^3CT(\text{Carb} \rightarrow \text{DAC})$ and ${}^3LE(\text{DAC})$ ): 3.82eV = 325nm	HOMO-3 – LUMO (40%)	

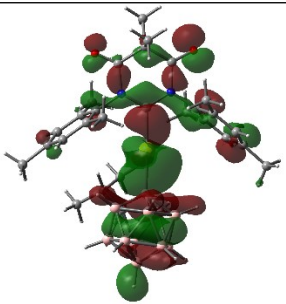
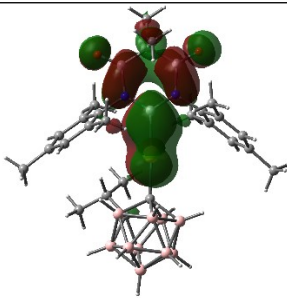
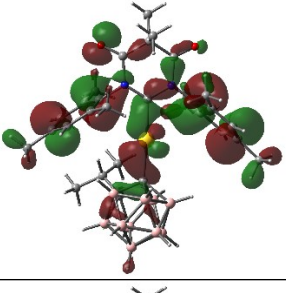
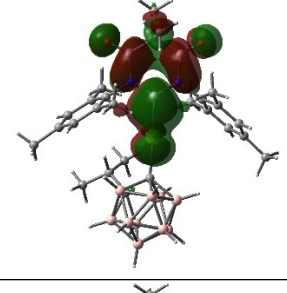
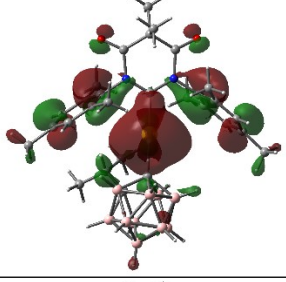
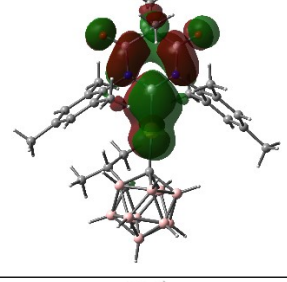
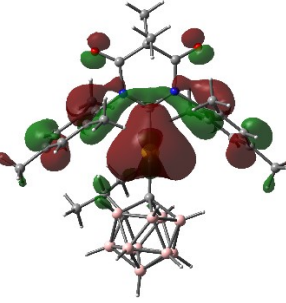
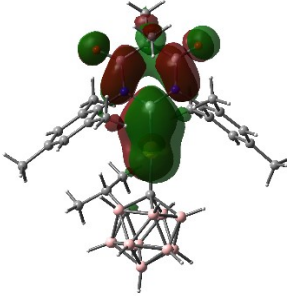
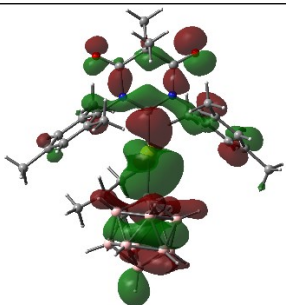
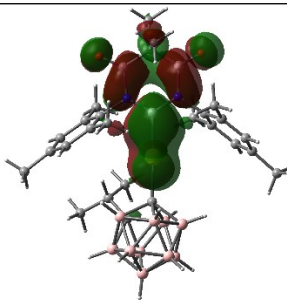
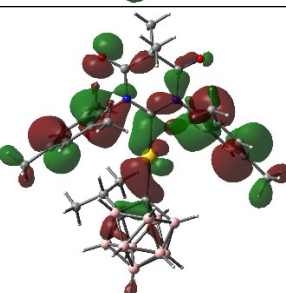
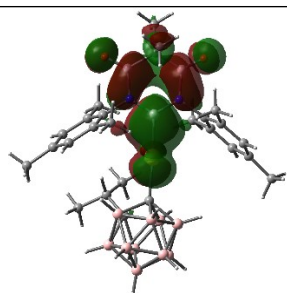
**Table S8.** Optimized excited states energetics.

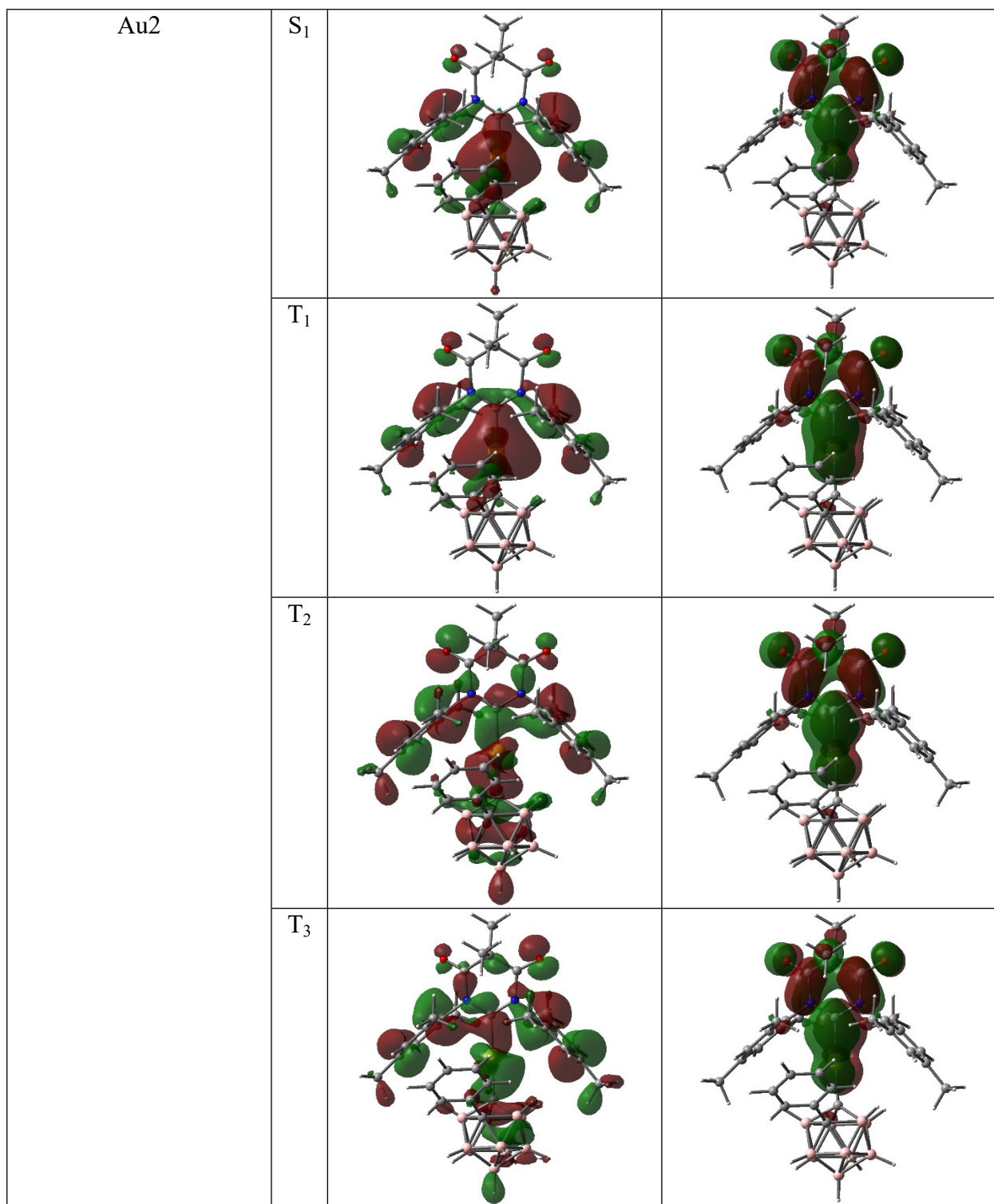
	Fluorescence ( $S_1-S_0@S_1$ )	Phosphorescence ( $T_1-S_0@T_1$ )	Oscillator strength for fluorescence		
Au1	2.51eV = 494nm	2.32eV = 535nm	0.0022		
Au2	2.48eV = 501nm	2.30eV = 539nm	0.0028		
Au3	2.62eV = 473nm	3.42eV = 513nm	0.0025		
Cu1	2.11eV = 587nm	1.99eV = 624nm	0.0027		
Cu2	2.20eV = 564nm	1.96eV = 634nm	0.0068		
	Energies relative to optimized $S_0$				
	Optimized $S_1$		Optimized $T_1$		$\Delta E_{ST}$ (eV)
	kJ/mol	eV	kJ/mol	eV	
Au1	287.3	2.98	269.8	2.80	0.18
Au2	285.0	2.95	265.7	2.75	0.20
Au3	289.0	3.00	268.3	2.78	0.22
Cu1	256.5	2.66	229.4	2.38	0.28
Cu2	248.1	2.57	219.9	2.28	0.29

**Table S9.** Natural transition orbitals NTO for vertical excited  $S_1$ ,  $T_1$ ,  $T_2$  and  $T_3$  states.

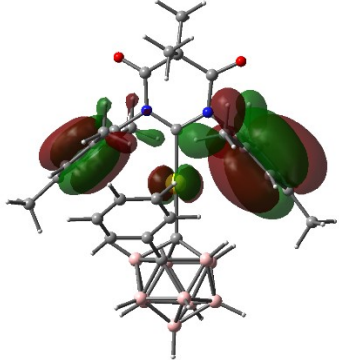
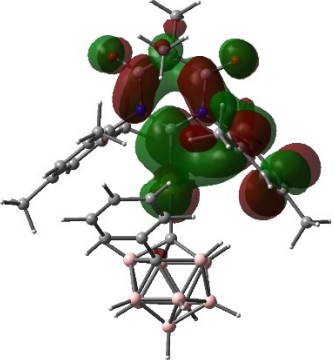
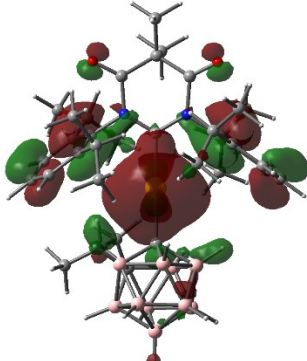
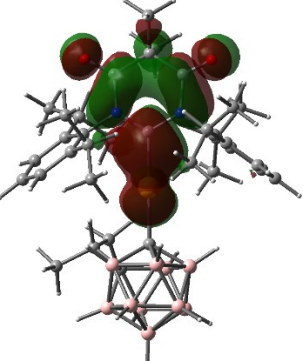
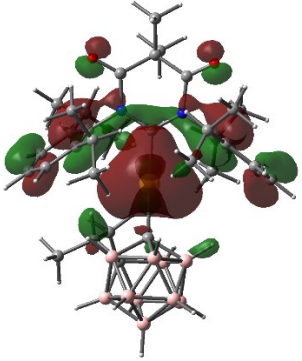
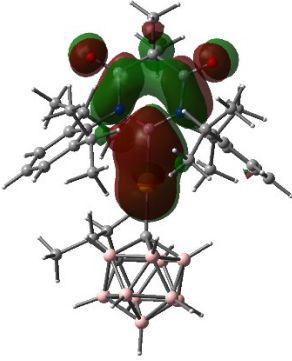
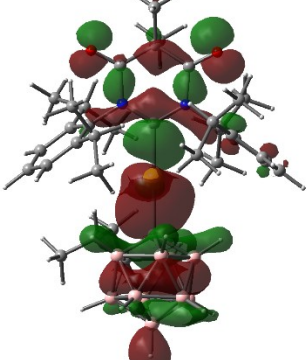
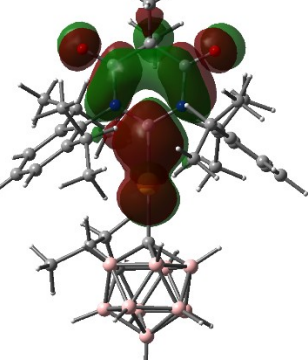
		HONTO	LUNTO
Au1 (crystal)	$S_1$		
	$T_1$		

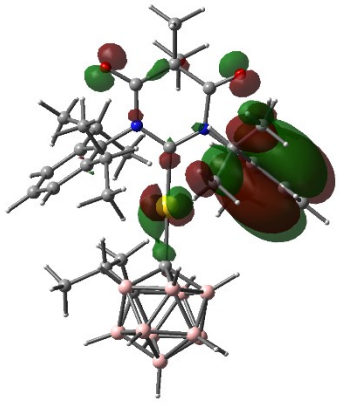
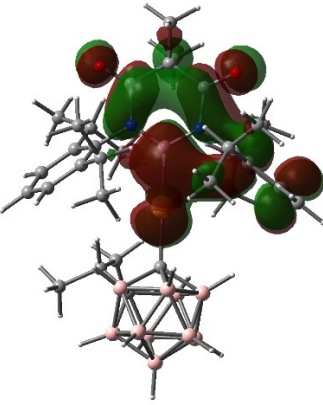
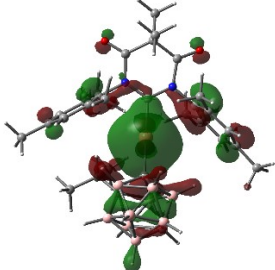
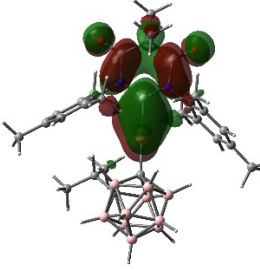
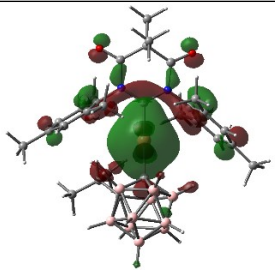
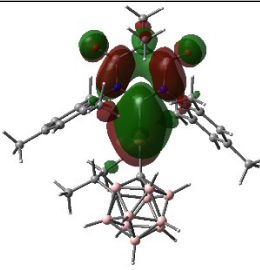
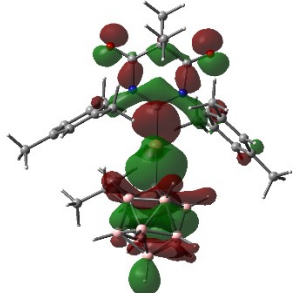
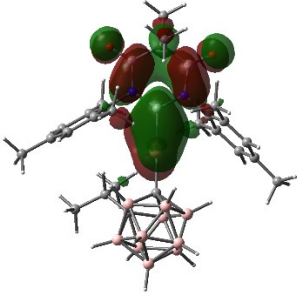
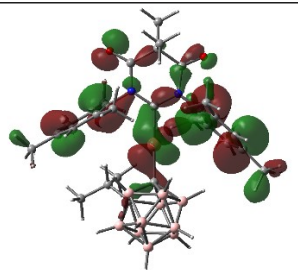
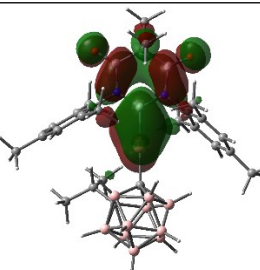


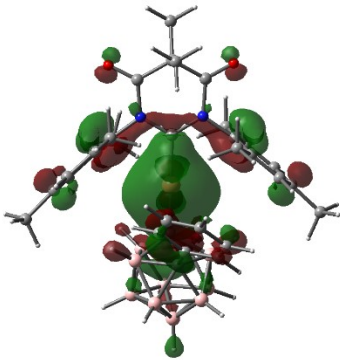
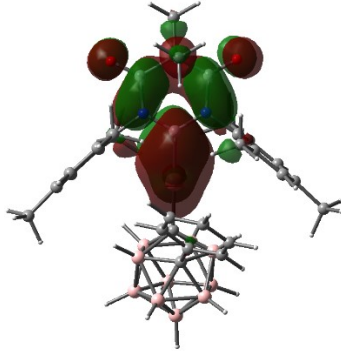
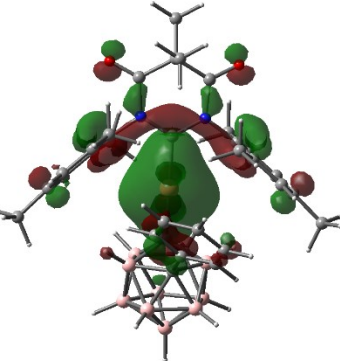
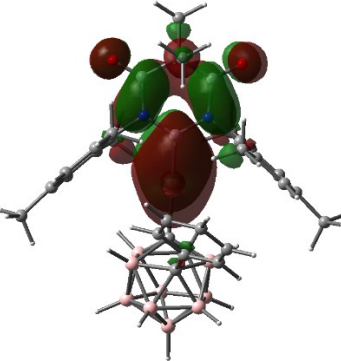
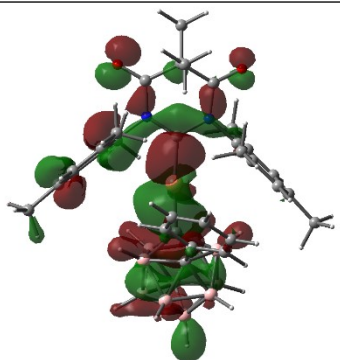
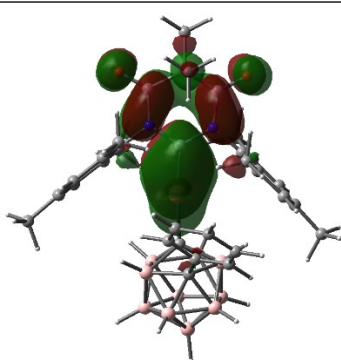
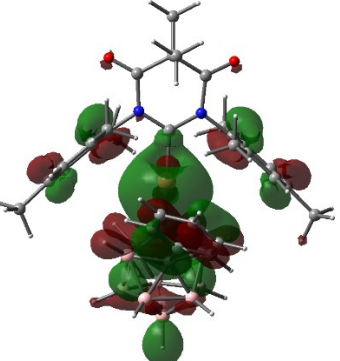
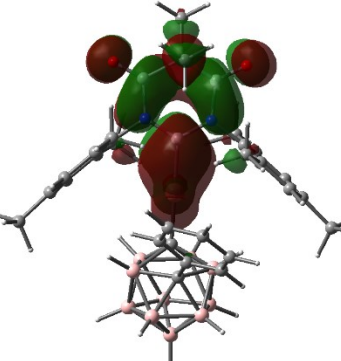
	T <sub>2</sub>		
	T <sub>3</sub>		
Au1 (opt-S0)	S <sub>1</sub>		
	T <sub>1</sub>		
	T <sub>2</sub>		
	T <sub>3</sub>		





	T <sub>4</sub>		
Au <sub>3</sub>	S <sub>1</sub>		
	T <sub>1</sub>		
	T <sub>2</sub>		

	T <sub>3</sub>		
CuI	S <sub>1</sub>		
	T <sub>1</sub>		
	T <sub>2</sub>		
	T <sub>3</sub>		

Cu2	S <sub>1</sub>		
	T <sub>1</sub>		
	T <sub>2</sub>		
	T <sub>3</sub>		

---

**References**

- 
- [1] A. Toppino, A. F. Genady, M. E. El-Zaria, J. Reeve, F. Mostofian, J. Kent, J. F. Valliant, *Inorg. Chem.*, **2013**, 52, 15, 8743-8749.
- [2] K. Arumugam, B. Varghese, J. N. Brantley, S. S. M. Konda, V. M. Lynch, C. W. Bielawski, *Eur. J. Org. Chem.*, **2014**, 493-497.
- [3] L. R. Collins, J. P. Lowe, M. F. Mahon, R. C. Poulten, M. K. Whittlesey, *Inorg. Chem.*, **2014**, 53, 5, 2699-2707.
- [4] G. Gritzner, J. Kůta, Recommendations on reporting electrodepotentials in nonaqueous solvents: IUPC commission on electro-chemistry. *Electrochim. Acta*, 1984, 29, 869–873.
- [5] Programs CrysAlisPro, Oxford Diffraction Ltd. Abingdon, UK, 2010.
- [6] G. Sheldrick, Crystal structure refinement with SHELXL. *Acta Cryst. C*, **2015**, 71 (1), 3-8.
- [7] G. Sheldrick, SHELXT - Integrated space-group and crystal-structure determination. *Acta Cryst. A*, **2015**, 71 (1), 3-8.
- [8] O.V. Dolomanov, L. J. Bourhis, R. J. Gildea, J. A. K. Howard, H. Puschmann, OLEX2: a complete structure solution, refinement and analysis program. *J. Appl. Cryst.*, **2009**, 42 (2), 339-341.
- [9] F. Furche, D. Rappoport, Density functional methods for excited states: equilibrium structure and electronic spectra. In *Computational Photochemistry*; M. Olivucci, Ed.; Elsevier: Amsterdam, 2005; pp. 93–128.
- [10] M. J. G. Peach, D. J. Tozer, *J. Phys. Chem. A*, **2012**, 116, 9783–9789.
- [11] Gaussian 16, Revision A.03, M.J. Frisch, G.W. Trucks, H.B. Schlegel, G.E. Scuseria, M.A. Robb, J.R. Cheeseman, G. Scalmani, V. Barone, G.A. Petersson, H. Nakatsuji, X. Li, M. Caricato, A.V. Marenich, J. Bloino, B.G. Janesko, R. Gomperts, B. Mennucci, H.P. Hratchian, J.V. Ortiz, A.F. Izmaylov, J.L. Sonnenberg, D. Williams-Young, F. Ding, F. Lipparini, F. Egidi, J. Goings, B. Peng, A. Petrone, T. Henderson, D. Ranasinghe, V.G. Zakrzewski, J. Gao, N. Rega, G. Zheng, W. Liang, M. Hada, M. Ehara, K. Toyota, R. Fukuda, J. Hasegawa, M. Ishida, T. Nakajima, Y. Honda, O. Kitao, H. Nakai, T. Vreven, K. Throssell, J.A. Montgomery, Jr., J.E. Peralta, F. Ogliaro, M.J. Bearpark, J.J. Heyd, E.N. Brothers, K.N. Kudin, V.N. Staroverov, T.A. Keith, R. Kobayashi, J. Normand, K. Raghavachari, A P. Rendell, J.C. Burant, S.S. Iyengar, J. Tomasi, M. Cossi, J.M. Millam, M. Klene, C. Adamo, R. Cammi, J.W. Ochterski, R.L. Martin, K. Morokuma, O. Farkas, J.B. Foresman, D.J. Fox, Gaussian, Inc., Wallingford CT, **2016**.
- [12] F. Weigend, M. Häser, H. Patzelt, R. Ahlrichs, *Chem. Phys. Lett.*, **1998**, 294, 143–152.
- [13] F. Weigend, R. Ahlrichs, *Phys. Chem. Chem. Phys.*, **2005**, 7, 3297–3305.

- 
- [14] D. Andrae, U. Haeussermann, M. Dolg, H. Stoll, H. Preuss, *Theor. Chim. Acta*, **1990**, *77*, 123–141.
- [15] See e.g. N. Le Phuoc, A.C. Brannan, A.S. Romanov, M. Linnolahti, *Molecules*, **2023**, *28*, 4398. and references therein.
- [16] T. Lu, F. Chen, *J. Comput. Chem.*, **2012**, *33*, 580–592.